NITROGEN SPECIES IN THE POST-PINATUBO STRATOSPHERE: MODEL ANALYSIS UTILIZING UARS MEASUREMENTS

by

M.Y. Danilin[1], J.M. Rodriguez[1], W. Hu[1], M.K.W. Ko[1],
D.K. Weisenstein[1], J.B. Kumer[2], J.L. Mergenthaler[2],
J.M. Russell III[3], M. Koike[4], and G.K. Yue[5]

[1]AER, Inc., 840 Memorial Drive, Cambridge, MA 02139

[2] Lockheed Palo Alto Research Laboratory, Palo Alto, CA 94304

[3] Department of Physics, Hampton University, Hampton, VA 23668

[4] Solar-Terrestrial Environmental Laboratory, Nagoya University, Japan

[5] NASA Langley Research Center, Hampton, VA 23681

Submitted to Journal of Geophysical Research

September 14, 1998

Abstract

We present an analysis of the impact of heterogeneous chemistry on the partitioning of nitrogen species measured by the Upper Atmosphere Research Satellite (UARS) instruments. The UARS measurements utilized include: N_2O, HNO_3 and $ClONO_2$ (Cryogen Limb Array Etalon Spectrometer (CLAES), version 7), temperature, methane, ozone, H_2O, HCl, NO and NO_2 (HALogen Occultation Experiment (HALOE), version 18). The analysis is carried out for the data from January 1992 to September 1994 in the 100-1 mbar (~17-47 km) altitude range and over 10 degree latitude bins from 70°S to 70°N. Temporal-spatial evolution of aerosol surface area density (SAD) is adopted according to the Stratospheric Aerosol and Gas Experiment (SAGE) II data. A diurnal steady-state photochemical box model, constrained by the temperature, ozone, H_2O, CH_4, aerosol SAD and columns of O_2 and O_3 above the point of interest, has been used as the main tool to analyze these data. Total inorganic nitrogen (NO_y) is obtained by three different methods: 1) as a sum of the UARS measured NO, NO_2, HNO_3, and $ClONO_2$; 2) from the N_2O-NO_y correlation, 3) from the CH_4-NO_y correlation. To validate our current understanding of stratospheric heterogeneous chemistry for post-Pinatubo conditions, the model-calculated NO_x/NO_y ratios and the NO, NO_2, and HNO_3 profiles are compared to the UARS-derived data. In general, the UARS-constrained box model captures the main features of nitrogen species partitioning in the post-Pinatubo years. However, the model underestimates the NO_2 content, particularly, in the 30-7 mbar (~ 23-32 km) range. Comparisons of the calculated temporal behavior of the partial columns of NO_2 and HNO_3 and ground based measurements at 45°S and 45°N are also presented. Our analysis indicates that ground-based and HALOE v.18 measurements of the NO_2 vertical columns are consistent within the range of their uncertainties and are systematically higher (up to 50%) than the model results at mid-latitudes in both hemispheres. Reasonable agreement is obtained for HNO_3 columns at 45°S suggesting some problems with nitrogen species partitioning in the model. Outstanding uncertainties are discussed.

1. Introduction

Prior to the launch of the Upper Atmosphere Research Satellite (UARS) in September 1991, nitrogen species in the stratosphere had been sampled by several different platforms: aircraft (e.g. recent aircraft campaigns are summarized in the following special issues: *J. Geophys. Res., 94,* 1989, nos. D9 and D14; *97,* 1992, no. D8; *102,* 1997, D3; *Science, 261,* 1128-1158, 1993; *Geophys. Res. Lett., 17,* no.4, 1990; *23,* no.23, 1994), balloons [e.g. *Ridley et al.*, 1984, 1987; *Kondo et al.*, 1996,1997; *Jucks et al,* 1996; *Renard et al.,* 1996,1997; *Osterman et al.*, 1997; *Sen et al,* 1998], ground-based [e.g. *McKenzie et al.*, 1991; *Johnston et al.*, 1992; *Koike et al.*, 1993, 1994, 1998], limb infrared monitor of the stratosphere (LIMS) satellite [e.g. *Gille et al.*, 1984; *Russell et al.* 1984], and the atmospheric laboratory for applications and science (ATLAS) series of Shuttle missions [e.g. *Kaye and Miller*, 1996; *Rinsland et al.,* 1994]. The aircraft measurements revealed many interesting features of the nitrogen species behavior in the stratosphere, for example, saturation of the NO_x/NO_y ratio as a function of aerosol surface area above $\sim$5 $\mu m^2/cm^3$ [*Fahey et al.,* 1993] and denitrification in polar stratospheric cloud (PSC) regions [*Fahey et al.*, 1990]. However, such measurements are limited by the ER-2 ceiling altitude ($\sim$20 km), and their coverage is limited by aircraft paths and duration of flights. The balloon measurements mentioned can provide vertical profiles of several species up to 60 km [*Osterman et al.*, 1997], but, again, these data have very limited coverage. The ground-based measurements of NO_2 and HNO_3 give the vertical profiles and column values of these species [*McKenzie et al.*, 1991; *Nolholt,* 1994; *Johnston et al.*, 1992; *Koike et al.,* 1993, 1994]. Such measurements could provide long data sets, however, they are limited to particular stations and their analysis could be affected by prevailing local meteorological conditions. The LIMS sampling has given a near-global picture of temperature, ozone, H_2O, NO_2, and HNO_3 distributions during the October 1978-May 1979 period, which has been useful in validating global photochemical models [*Jackman et al.*, 1987; *Rood et al.,* 1993]. The ATLAS series provide the most comprehensive set of atmospheric species sampled, but these data have a limited temporal coverage (8-11 days) [*Kaye and Miller*, 1996].

Several special issues [see *Geophys. Res. Lett., 19,* 1992, no.2 and *20,* 1993, no.12, *J. Geophys. Res., 98,* 1993, no.D6 and *101,* 1996, no.D6, *J. Atmos. Sci., 52,* 1995, no.17] have dis-

cussed different aspects of the UARS measurements. Recently, *Dessler et al.* [1998] summarize principal scientific findings from the first five years of the UARS program. The UARS measurements provide a unique data set of key atmospheric species to be used for comparison of different satellite measurement techniques and validation of existing models of the atmosphere [*Reber et al.,* 1993]. The multi-year data sets of some UARS instruments (e.g. HALOE, MLS) provide not only pictures of the seasonal variability of some key stratospheric species on a near-global basis, but also an opportunity to investigate their inter-annual changes and trends.

Since the UARS was launched about three months after the Mt. Pinatubo eruption, there is an additional opportunity for atmospheric scientists to observe a near-global picture of the response of the atmosphere to the strongest natural perturbation in this century. Many modeling efforts have been undertaken to estimate different atmospheric effects of the Pintaubo aerosol [*Boville et al.,* 1991; *Brasseur and Granier,* 1992; *Pitari and Rizi,* 1993; *Bekki and Pyle,* 1994; *Kinnison et al.,* 1994; *Rodriguez et al.*, 1994; *Tie et al.,* 1994; *Solomon et al.,* 1996; *Rosenfield et al.,* 1997; *Weisenstein et al.*, 1997]. Additionally, the ground-based measurements detected the increase of HNO_3 and decrease of NO_2 columns after the Pinatubo eruption [*Johnston et al.*, 1992; *Koike et al.*, 1993,1994; *David et al.,* 1994; *Preston et al.,* 1997; *Slusser et al.*, 1997, 1998; *Van Roozendael et al.,* 1997], which could be explained by the considerably enhanced N_2O_5 and $BrONO_2$ hydrolysis on the Pinatubo aerosol. The HNO_3 and NO_2 responses to the Pinatubo eruption are consistent with the model predictions qualitatively. However, the magnitude of the observed perturbations of the HNO_3 and NO_2 columns at 45°S are almost two-fold stronger than the calculated effect by the LLNL, AER, and GSFC 2-D models [*Koike et al.*, 1994; *Rosenfield et al.,* 1997].

We utilize UARS data to investigate whether the observed NO_x/NO_y, NO, NO_2, and HNO_3 distributions under the wide range of aerosol loading in the post-Pinatubo stratosphere are consistent with those predicted by our model calculations. We focus our study here to analysis of the nitrogen species only, since they play an important role for the photochemical ozone balance in the stratosphere. Detailed analysis of the chlorine species partitioning has been done by *Dessler et al.* [1995,1996]. Our related study [*Hu et al.,* 1998] will discuss the ozone photochemical tendencies in the stratosphere as seen by UARS. This paper shows our model analysis

of the UARS data acquired and incorporated in our data set. In the next section the approach used and model initialization are discussed. In section three we present results for the vertical profiles of nitrogen species, while the next section is about comparison of the column data of NO_2 and HNO_3. Finally, the last section summarizes our major findings.

2. Approach and Model Constraints

2.1. Approach

A diurnal steady-state version of the AER box model without PSC chemistry is used to calculate the concentrations of trace species. Previous analysis of aircraft data [*Salawitch et al.*, 1994; *Gao et al*, 1997] shows that steady-state photochemical models can be applied almost everywhere in the stratosphere successfully, except in PSC processing regions or regions with temperature changes larger than 10-15 K/day [*Kawa et al.*, 1993]. A list of the included heterogeneous reactions on sulfate aerosol is given in Table 1 with the updated $BrONO_2 + H_2O$ reaction probability equals to γ=1/(1/0.88 + 1/exp(17.832-0.245wt%)) according to *D.R. Hanson*, [personal communication] (wt% is the weight percent of H_2SO_4 in sulfate aerosol). This change should be noticed in the context of this paper, since the new values of γ are larger than those in *Hanson et al.* [1996] by 0.3-0.4 and the $BrONO_2$ hydrolysis is not saturated even at high volcanic aerosol loading, thus further reducing NO_x (=NO+NO_2) in the lower stratosphere [*Danilin and McConnell*, 1995; *Lary et al.*, 1996]. Other reaction rates are taken from *DeMore et al.* [1997].

The HALOE and CLAES instruments provide 30 and approximately 1300 individual vertical profiles per day, respectively. To perform calculations for each profile for the period from January 1992 to September 1994 would be an enormous task. As an alternative, we created merge files of the CLAES and HALOE data to represent zonal monthly or yaw-averaged conditions (see section 2.2). These files are used to provide input for the model runs. The measured species from these files are compared against the model results. To check the validity of this approach, we performed daily runs for February 1993. We picked this month because atmospheric circulation is perturbed at the end of the winter in the northern hemisphere, thus providing potentially a worst case scenario for our study. We calculate the monthly averaged NO_x/NO_y ratios using

our merge files as input. The value of $<\frac{NO_x}{NO_y}|_{daily}>$ averaged over the month is compared with a single calculation for the monthly averaged $<\frac{NO_x}{NO_y}>|_{monthly}$ at the same level and latitude bin.

Figure 1 depicts the relative difference of this comparison for $\frac{<\frac{NO_x}{NO_y}|_{daily}>-<\frac{NO_x}{NO_y}>|_{monthly}}{<\frac{NO_x}{NO_y}|_{daily}>}$ (in %). Data in the northern and southern hemispheres correspond to HALOE sunset and sunrise measurements, respectively. In general, the difference between daily and monthly runs is in the ±10% range almost everywhere, except for some points in the lower stratosphere. We analyzed the most striking points where the difference was above the ±10% range. Our analysis of these points (not shown here) reveals that the individual daily NO_x/NO_y ratios could be very scattered. For example, among 15 individual HALOE measurements on February 22 and 23 at 15°N and 68 mb, 4 measurements give $NO_x/NO_y \sim 0.25$, 7 measurements between 0.17 and 0.2, 4 measurements show very low NO_x/NO_y <0.05 (thus giving $< \frac{NO_x}{NO_y}|_{daily} >=0.16$), while $< \frac{NO_x}{NO_y} > |_{monthly}=0.2$. The other points outside the 10% difference range in Figure 1 are also characterized by a large scattering of individual HALOE measurements. Our conclusion from this comparison is that: 1) our approach using monthly averaged merge files is reasonable for the purpose of this study and 2) analysis of the individual UARS profiles, if necessary, should be done very cautiously, especially in the lower stratosphere, where the accuracy of individual measurements could be low (15% for HALOE NO and NO_2, 6-15% for CLAES HNO_3, 23% for CLAES $ClONO_2$ [*Morris et al.*, 1997; Table 1]) and less data may be available.

2.2. UARS Merged Data

We created a merged UARS data set containing the zonally-averaged stratospheric trace species on daily, monthly and yaw-averaged (i.e. during the 36-day yaw cycle) bases. Daily CLAES v.7 measurements released on CD-ROMs and the recently released v.18 of the HALOE data are used to create these merge files. The files contain measured concentrations of the following species: HALOE CH_4, NO, NO_2, H_2O, O_3, HCl, and temperature; CLAES N_2O, HNO_3, $ClONO_2$, and N_2O_5; at the following 13 pressure levels: 100, 68.2, 46.4, 31.6, 21.5, 14.7, 10, 6.8, 4.6, 3.2, 2.2, 1.5, and 1 mbar. The daily files simply summarize available HALOE measurements and CLAES data within ±5° latitude and ±10° longitude distance from a HALOE point during a particular day at these levels.

There are 10 yaw-averaged files per year, since the duration of a yaw cycle is approximately 36 days. We bin the data by latitude with a 10^o step from 70^oS to 70^oN and mark the UARS results by a mean latitude value in each bin (i.e. 65^oS corresponds to the 70^oS-60^oS band etc.). Available UARS data beyond the 70^oS-70^oN range (namely, 80^oS-70^oS and 70^oN-80^oN) are ignored because of the following two reasons: first, they are rather sparse and cannot provide enough coincident measurements by the CLAES and HALOE instruments in a 10^o bin due to their sampling geometry; second, our diurnal steady-state model approach may be less valid in these regions, especially after polar vortex breakups. The HALOE measurements for each yaw cycle and latitude bin are averaged, thus forming a skeleton of the merge files for the sunrise and sunset data, separately. Only those CLAES daily measurements that are within 5^o latitude distance from a HALOE sampling on the same day are selected for the yaw-averaged files. They are included in the merge files after simply zonally averaging. This approach should be robust for the long-lived species, like HNO_3 and N_2O. Possible errors in $ClONO_2$ data (its diurnal variability could contribute only 3% at most in NO_y [*Morris et al.*, 1997]) have a negligible effect on the conclusions of this study. Performing a similar analysis, *Morris et al.* [1997] concluded that a more sophisticated method (like trajectory mapping technique [*Morris et al.*, 1995]) is not necessary for such kinds of studies, since the zonal averaged data provide almost the same results. Each yaw-averaged merge file also contains variances of the measured parameters during a yaw cycle.

The same approach is used to create monthly zonally averaged merge files. Additionally, we created files of zonally monthly averaged CLAES measurements of N_2O, HNO_3, and $ClONO_2$, disregarding their proximity to the HALOE points. These files of nitrous oxide zonally averaged data $<N_2O^c>$ are used to calculate NO_y, Cl_y, and Br_y to initialize our box model runs for the N_2O approach. Our analysis is focused below on the zonally averaged merge files created for each yaw cycle from January 1992 to September 1994 and related to the sunset and sunrise HALOE measurements.

2.3. Model Constraints

We initialize our calculations with H_2O, CH_4, and O_3 data from the yaw-averaged merge

files described above. Ozone is kept constant in the model a id equal to its HALOE value. Our merge files contain also SAGE II aerosol SAD, ozone and oxygen columns above each level, and averaged julian day of the HALOE measurements to calculate photolysis rates. To calculate diurnal behavior of the solar zenith angle, solar declination is adopted for the mean day of the HALOE measurements for the yaw cycle and latitude bin considered. The ozone column above the point of interest is obtained by integrating the available HALOE ozone profile for that particular latitude and month. The O_2 column is defined by the pressure level of interest p as O_2^{column} (cm^{-2}) = $4.444 \times 10^{21} \times$p (in mbar).

Since we are running our box model until steady-state conditions, initial partitionings within NO_y, Cl_y and Br_y families are not important. However, UARS does not measure all nitrogen, chlorine and bromine species required to constrain total inorganic nitrogen (NO_y), inorganic chlorine (Cl_y), and inorganic bromine (Br_y) for the model runs, so methods of model initialization are needed. Three alternative methods to constrain these families are outlined in Table 2 and discussed in the following subsections.

2.3a. NO_y

The first way is to define total nitrogen NO_y (= NO + NO_2 + NO_3 + HNO_3 + 2×N_2O_5 + HONO + HNO_4 + $ClONO_2$ + $BrONO_2$) as $NO_y^U = < NO^J > + < NO_2^U > + < HNO_3^U > + < ClONO_2^U >$, where the superscript U denotes UARS measurements of NO, NO_2 (by HALOE), HNO_3, and $ClONO_2$ (by CLAES), and the symbol <> denotes zonally averaged value of the bracketed species during a yaw cycle. We did not include CLAES N_2O_5 in the equation for NO_y (since these measurements are recommended for use only at 3.2, 2.2, and 1.5 mbar [*Kumer et al.*, 1996b]), thus underestimating NO_y in this approach The other omitted species in the equation for NO_y^U (NO_3, HONO, HNO_4, $BrONO_2$) may contribute only a few percent or less to NO_y, and thus are unimportant for the purposes of this study.

The second approach is to use zonally averaged values of CLAES $<N_2O^c>$ to derive NO_y using equation (1) in the northern hemisphere by *Loewenstein et al.*, [1993] and equation (2) in the southern hemisphere by *Keim et al.* [1997]:

$$NO_y = 20.7 - 0.0644 \times N_2O, \quad (1)$$

$$NO_y = 21.82 - 0.0699 \times N_2O, \quad (2)$$

in the above equation NO_y and N_2O are in ppbv. These empirical N_2O-NO_y correlations are valid for $N_2O \geq 50$ ppbv (below ~10 mbar) [*Fahey et al.*, 1990; *Prather and Remsberg,* 1993]. Above this altitude, destruction of NO_y via photolysis of NO followed by the N + NO$\longrightarrow$ N_2 + O reaction cause the correlation curve to turn over. Above these altitudes, we use NO_y^U or utilize the correlations derived from ATMOS (see Figure 2 and discussion below). These two approaches can be used to initialize our box model only until May 1993, since the CLAES cryogen supply was exhausted after that time.

The third method, which uses the HALOE measurements of CH_4, allow us to extend our model analysis after May 1993. This approach uses the empirical correlation between NO_y, N_2O, and CH_4 based on the analysis of ATLAS/ATMOS data [*Michelsen et al.*, 1998]. Their analysis provides two sets of the equations:

in the tropics (i.e. between 20°S and 20°N) for 0.4 ppmv $\leq CH_4 \leq$ 1.28 ppmv:

$NO_y = -1.3519\times10^{-8} + 0.05794(CH_4) - 18544(CH_4)^2 - 7.3339\times10^{9}(CH_4)^3$,

for $CH_4 >$ 1.28 ppmv:

$NO_y = -7.9107\times10^{-7} + 1.4051(CH_4) + 8.3839\times10^{5}(CH_4)^2 - 1.6787\times10^{11}(CH_4)^3$,

and outside tropics for $CH_4 <$0.9 ppmv:

$NO_y = -1.2321\times10^{-9} + 0.02276(CH_4) - 31866(CH_4)^2 - 4.178\times10^{10}(CH_4)^3$;

for $CH_4 \geq$0.9 ppmv:

$NO_y = 9.8251\times10^{-9} + 0.0418(CH_4) - 55088(CH_4)^2 + 1.608\times10^{10}(CH_4)^3$,

here NO_y and CH_4 are in mixing ratio. We must stress the approximate nature of these correlations. They do not account for possible latitudinal and seasonal changes, which could be particularly important at higher altitudes [*Keim et al.*, 1997]. There are several situations when the HALOE NO_x measured at higher altitudes (where NO_x is the major NO_y component) is larger than the NO_y derived from the CH_4 correlations. In these cases, the initial NO_y is assigned to be equal to $NO_x^{HALOE} + HNO_3^{CLAES} + ClONO_2^{CLAES}$ or to NO_x^{HALOE} (if CLAES data are not available).

Figure 2 compares the NO_y fields in January 1993 calculated from the three methods outlined above. This month is chosen for illustration because it contains the largest latitudinal coverage by the sunset UARS measurements. The top panel shows NO_y^U (= HALOE sunset

monthly zonally averaged values of <NO> and <NO_2 > together with CLAES <HNO_3> and <$ClONO_2$>). The middle panel depicts the difference between NO_y, inferred from the zonal yaw-averaged N_2O field by CLAES <N_2O^c>, and NO_y^U. The bottom panel shows the difference between NO_y, obtained according to the above CH_4-NO_y correlation for the HALOE <CH_4>, and NO_y^U. In general, all three approaches have similar features: relatively low NO_y values in the lower stratosphere, especially in the tropics; gradual increase with altitude up to the maximum values above 20 mbar and decrease above 3 mbar. However, more detailed analysis also reveals principal differences in these NO_y fields. For example, the CH_4 approach (bottom panel) gives the highest level of NO_y with its maximum above 18 ppbv (i.e. 1-2 ppbv higher than NO_y^U) in the tropics at 10-3 mbar (~34-40km). Compared to NO_y^U, the CH_4 approach overestimates the NO_y content up to 3 ppbv in the upper stratosphere in the tropics, near the tropical barrier and winter mid-latitudes up to 3 ppbv and underestimates up to 3 ppbv above 2 mbar in the summer mid-latitudes. Switching from tropical to extratropical CH_4-NO_y correlations, we see some problems near 20°S and 20°N (lower panel). The N_2O approach (middle panel) shows, in general, a good agreement with the UARS approach. However, somewhat larger NO_y mixing ratios (>1 ppbv) are obtained below 40 mbar at southern mid-latitudes due to low values of CLAES N_2O there. Also, the N_2O method provides smaller NO_y values than those in the UARS approach by >1 ppbv (middle panel) between 10-7 mbar in the tropics. Above 7 mbar, the NO_y contents are the same for the N_2O and UARS approaches. Obviously, the UARS approach has the smallest altitudinal-latitudinal coverage below 30 mbar (since it requires almost coincident measurements of *all* four species: NO, NO_2, HNO_3, and $ClONO_2$, while the other methods require only N_2O^{CLAES} and CH_4^{HALOE}), thus potentially leaving more gaps in the model analysis. In general, the three approaches give reasonably close results at mid-latitudes. The largest discrepances are observed in the tropics and subtropics and in the upper stratosphere, maybe due to a combination of interference from Pinatubo aerosols and poorly defined tracer-tracer correlations.

Our analysis of similar plots for other months and years shows that the above mentioned differences and similarities of the NO_y field are persistent. For example, figure 3 show the difference between NO_y distribution during the first yaw cycles (mostly occurred in January)

in 1992 and 1993 defined by the UARS (top panel), CLAES N_2O (middle panel), and HALOE CH_4 (bottom panel) methods. This figure depicts the change in atmospheric dynamics from January 1992 to January 1993 (since NO_y could serve as a tracer) and compares three methods to define NO_y. There are the following similarities: higher values of NO_y in January 1992 below 10-20 mbar (30-40 mbar) in the southern (northern) mid-latitudes; higher NO_y content above 2 mbar in the tropics in January 1992. Among the differences, one can mention stronger change of NO_y below 40 mbar at northern and southern mid-latitudes and different values of NO_y change between 30°S and 40°N at the pressure range of 30-5 mbar in the CH_4 scheme.

Since the UARS does not measure NO_y itself, Figures 2-3 illustrate only the quality of the above correlations and, strictly speaking, cannot conclude which approach is right. In general, NO_y derived directly from UARS is preferable in the lowermost stratosphere, provided that the error bars for individual components are not too large. The UARS initialization of NO_y is preferable in the upper stratosphere, since the N_2O-NO_y and CH_4-NO_y correlations are less reliable there. Initialization of NO_y from the output of a global model for a particular location, season, and altitude could introduce additional uncertainties due to model formulations of dynamics and chemistry. For example, *Nevison et al.* [1997] reported that the Garcia-Solomon model overestimates NO_y in the upper stratosphere.

Our sensitivity study shows that *the model NO_x/NO_y ratio is insensitive to NO_y*, changing roughly a couple percent per 10-20% of NO_y change. This helps us to ignore possible uncertainties of the NO_y initialization, analyzing the NO_x/NO_y behavior.

2.3b. Cl_y and Br_y

Initial inorganic chlorine Cl_y (=HCl + $ClONO_2$ + HOCl+ Cl + ClO + BrCl + 2(Cl_2 + Cl_2O_2)) is defined from the correlation of total (organic and inorganic) chlorine with N_2O [*Woodbridge et al.*, 1995; their equation (11)] and dependence of the Cl_y fraction of total chlorine as a function of N_2O [their Figure 7]. The initial values of inorganic bromine Br_y (= Br + BrO + HOBr + $BrONO_2$ + BrCl + HBr + 2Br_2) are inferred from the empirical correlation of Br_y with N_2O [*R.J. Salawitch, personal communication*, 1997]:

for 120 ppbv$\leq N_2O \leq$ 312 ppbv:

$$Br_y = 13.009 + 0.1284(N_2O) - 5.452 \times 10^{-4}(N_2O)^2, \quad (3)$$

for $N_2O \leq$ 120 ppbv:

$$Br_y = 21.0984 - 0.5317(N_2O/120) \quad (4)$$

where Br_y is in pptv and N_2O is in ppbv (Br_y=1 pptv is assumed at N_2O> 312 ppbv). These values of Br_y could differ by up to 2 pptv from the recent analysis by *Wamsley et al.* [1998] in the stratosphere. However, this potential difference is not important for the analysis of nitrogen species presented here. To calculate the Cl_y and Br_y contents, the N_2O values could be obtained from the yaw-averaged CLAES <N_2O^c> data before May 1993 or HALOE data of <CH_4 > after May 1993 using the CH_4-N_2O correlation [*Michelsen et al.*, 1998]:

in the tropics (i.e. 20°S-20°N):

$N_2O^* = -1.2851\times10^{-7} + 0.7742(CH_4) - 1.5510\times10^{6}(CH_4)^2 + 1.3097\times10^{12}(CH_4)^3 - 3.3888\times10^{17}(CH_4)^4$;

outside the tropics:

$N_2O^* = -2.2309\times10^{-8} + 0.1934(CH_4) - 5.6278\times10^{5}(CH_4)^2 + 7.3019\times10^{11}(CH_4)^3 - 2.34\times10^{17}(CH_4)^4$,

here N_2O^* and CH_4 are in mixing ratio. The contents of inorganic chlorine and bromine species could be different for the two approaches, when both CLAES N_2O and HALOE CH_4 are available. However, the possible differences do not significantly affect nitrogen species partitioning investigated in this paper.

3. Analysis of Vertical Profiles of Nitrogen Species

3.1. NO_x/NO_y

We performed model runs for each yaw period from January 1992 to September 1994 for sunrise and sunset measurements, except for June 1992, when HALOE did not operate because of technical problems aboard the UARS. Latitudinal coverage of our merge files and, consequently, our model calculations differs from month to month, depending on the geometry of the HALOE and CLAES samplings. In this study we focus on analysis of the nitrogen species behavior primarily at 45°S and 45°N, since additional ground-based measurements of NO_2 and HNO_3 are available at these latitudes. Such a comparison of model calculations with measure-

ments obtained by two very different techniques should be a very useful test to analyze the representation of stratospheric chemistry in the models.

Figure 4 shows temporal evolution of the sunset NO_x/NO_y ratio and aerosol SAD at four levels: 68, 46, 31, and 22 mbar levels at 45°S (left column) and 45°N (right column). We show these levels because the lower stratosphere has the strongest perturbation due to Pinatubo aerosol [e.g. *Yue et al.*, 1994; *Lambert et al.*, 1997; *Thomason et al.*, 1997]. Results at the lowermost level of 100 mbar are not shown because the UARS measurements are very noisy due to retrieval problems within a dense Pinatubo aerosol cloud. Since the model NO_x/NO_y ratio is insensitive to the NO_y values, our model results are shown by red crosses in Figure 4 for the CH_4 approach only. However, since the UARS does not measure NO_y itself (while NO_x is measured by the HALOE instrument), there are differences between UARS NO_x/NO_y results because of the different ways to initialize NO_y according to the UARS (cyan symbols), N_2O (blue symbols), or CH_4 (green symbols) approaches. The principal differences between these initializations are already discussed in the previous section. The monthly variable deviations shown are derived from statistical analysis of the available UARS data at each level during a particular yaw period.

A seasonal modulation of the NO_x/NO_y ratio is clearly seen in both UARS data and model results. This ratio is maximum during summer (January at 45°S, June-July at 45°N) and minimum during winter (July at 45°S, January at 45°N) because of the increased photolysis of HNO_3 in summer and the increased heterogeneous processing via N_2O_5 hydrolysis in winter. Since there are many gaps in the UARS data set at this latitude, it is hard to see an interannual increase of the NO_x/NO_y ratio due to the shown reduction of SAD after the Pinatubo eruption. However, the NO_x recovery can be seen more clearly in the model results. Missing UARS points at 68 mbar during the first half of 1992 in Figure 4 are due to deterioration of the HALOE NO_x measurements by the Pinatubo aerosol at this level [*Gordley et al.*, 1996].

Comparison of the model and UARS results shows a good agreement at the 68 and 46 mbar levels throughout the whole period analyzed. However, at the upper levels (particularly, at 22 mbar), a clear underestimation of the NO_x/NO_y ratio by the box model in summer in both hemispheres is evident. At some points (January 1993 at 45°S and July 1992 at 45°N, 22 mbar)

this disagreement can be more than 30%. A similar problem was also noticed by *Morris et al* [1997; Plate 1], who applied the Goddard 2-D model with the UARS-constrained photochemistry and concluded that "the model NO_x/NO_y ratio is marginally but systematically lower than the UARS ratio, especially at 800K (~31 km) and 1000K (~35 km)". Recent analysis of the satellite [e.g., *Lary et al.*, 1997] and balloon measurements [*Sen et al.*, 1998; *Kondo et al.*, 1998] also show that current photochemical models with heterogeneous chemistry underestimate the NO_x amount in the stratosphere.

To investigate the altitudinal-latitudinal dependence of the NO_x/NO_y ratio, we present results in Figure 5 for January 1993 between 68 and 4.6 mbar. The UARS NO_x/NO_y ratio is shown by the cyan, blue and green symbols for the UARS, N_2O, and CH_4 approaches, respectively (see Table 1). The model values of NO_x/NO_y, calculated for the CH_4 approach, are shown by red and black lines for calculations with and without heterogeneous reactions on sulfate aerosol, respectively. Increase of the NO_x/NO_y ratio towards the summer hemisphere at all levels is due to faster photolysis of HNO_3 there. We performed model runs with gas phase chemistry only to investigate a sensitivity of the model NO_x/NO_y ratio to the heterogeneous reactions on sulfate aerosol. Recently, *Donahue et al.* [1997] argue that current recommendations [*DeMore et al.*, 1997] overestimate the HNO_3 formation reaction rates by 20-30%. Additionally, we run our model with heterogeneous reactions on sulfate aerosol and with the reduced by 25% reaction rate of $OH + NO_2 + M \longrightarrow HNO_3 + M$ (shown by the grey lines) to reflect the possibility outlined by *Donahue et al.* [1997], assuming that their data are valid for the stratospheric conditions.

The agreement between model calculations with heterogeneous chemistry and UARS measurements is reasonable below 31 mbar, especially in the winter (i.e. northern) hemisphere. In the summer (i.e. southern) hemisphere our model tends to underpredict the NO_x content at and above 46 mb. The gas phase chemistry results (black lines) clearly overestimate the NO_x/NO_y ratio at these levels. However, at three levels, 21.5, 14.7 and 10.0 mbar, model results with heterogeneous chemistry underestimate the NO_x/NO_y ratio by 0.1-0.2 at all latitudes. Even the NO_x/NO_y results for the gas phase chemistry runs fall below the measurements at 10 and 14.7 mbar everywhere and at 21.5 mbar at southern mid-latitudes. Since the aerosol SAD drops

with altitude, the difference between model results with and without heterogeneous chemistry is diminished at higher levels (black and red curves are coincident at 6.8 and 4.6 mb). At the two upper layers, 4.6 and 6.8 mbar, model results are consistent with the UARS measurements. The 25% reduction of the OH + NO_2 + M $\longrightarrow$ HNO_3 + M helps to increase the NO_x/NO_y ratio. However, this increase is still too small to explain the UARS measurements.

In our opinion, the most alarming signal for modelers from Figures 4 and 5 is a striking underprediction the NO_x/NO_y ratio in the lower and middle stratosphere, since predictive capabilities of global models could be affected, particularly, for tasks where accurate knowledge of NO and NO_2 at these altitudes are important or perturbations of interest include NO_x emissions (like aircraft).

3.2. NO, NO_2, HNO_3

To investigate model underestimation of the NO_x/NO_y ratio in the stratosphere more carefully, we analyze separately the sunset vertical profiles of NO, NO_2, and HNO_3 in January 1993 at 45°S (summer) and 35°N (winter) according to the UARS initialization (see Figure 6). The UARS values are shown by symbols, the box model profiles for the UARS approach by solid and dashed lines for calculations with and without heterogeneous reactions on sulfate aerosol, respectively. Below 30 mbar ($\sim$ 24 km) and above 6 mbar ($\sim$ 34 km), the model reproduces the observed profiles of these nitrogen species reasonably well. Results for N_2O_5 and $ClONO_2$ are not shown here, since 1) the maximum N_2O_5 mixing ratio at sunset is small (a few tenth of ppbv) due to its diurnal variability and 2) the $ClONO_2$ profile has a relatively small maximum ($\sim$ 1 ppbv at 20 mbar) which is properly reproduced by our model.

However, the box model considerably underestimates NO_2 and overestimates the HNO_3 amount in the 30-7 mbar range by several ppbv. The reason for this model underestimation is not clear yet and further analysis is required. Additional missing heterogeneous mechanism of renoxification on sulfate aerosol, like HNO_3 + H_2CO $\longrightarrow$ 2HONO + CO_2 + H_2O [*Fairbrother et al.*, 1997; *Iraci and Tolbert*, 1997] could barely help, since the sulfate aerosol SAD is small at these levels (e.g., <0.1 μ^2/cm^3 at 10 mbar in January 1993 at 45°S). Possible renoxification reactions on soot [*Tabor et al.*, 1994; *Rogaski et al.*, 1997; *Lary et al.*, 1997; *Bekki*, 1997] also

could not help, since there is not a noticeable amount of soot at these altitudes, according to current knowledge. Since results for the gas phase run (black lines) fall below the UARS data at 10 and 14.7 mbar, the heterogeneous chemistry could hardly be responsible for this disagreement. *Sen et al* [1998] also reported that the balloon measurements of NO_2 exceed the values calculated by the steady-state model by 20-30% at 15-30 km and this difference is larger than the estimated total uncertainty of the measurements. This disagreement could be reduced (but not solved!) by 10% changes of some photochemical constants (e.g. $NO+O_3 \longrightarrow NO_2 + O_2$ and NO_2 absorption cross section) within a given range of their uncertainties by [*DeMore et al.*, 1997]. Recent POLARIS campaign results show that photochemical models underpredict the NO_x amount in the lower stratosphere during summer under almost background aerosol loading [*R.J. Salawitch, personal communication*, 1998]. It is worth noticing that this model shortcoming in the altitude region between 30 and 7 mbar is responsible for consequent disagreement between models, on the one hand, and UARS and ground-base measurements, on the other hand, of the NO_2 columns (see next section). Perhaps something is missing in our current understanding of the gas phase or photolytic processes with nitrogen species at these levels. A careful look at the reaction rates crucial for the NO_x and HNO_3 partitioning is required. Additionally, *Zipf and Prasad* [1998] speculated that an oxygen molecule above 25 km could get excited by a photon in the Schumann-Runge bands and react in this excited short-lived state with N_2 producing two molecules of NO.

Since the HNO_3 content in the stratosphere is expected to increase after the volcanic eruptions due to enhanced N_2O_5 hydrolysis [*Rodriguez et al.*, 1991, 1994; *Brasseur and Granier*, 1992; *Bekki and Pyle*, 1994; *Kinnison et al*, 1994; *Risland et al.*, 1994], it is interesting to see how the CLAES HNO_3 distribution did react to the Pinatubo eruption to check for consistency between UARS and the model picture of this event. Figure 7 shows the change of the HNO_3 distribution between January 1992 and January 1993 as seen by the CLAES instrument (top panel) and as predicted by our model with heterogeneous reactions on sulfate aerosol for the UARS initialization (bottom panel). The corresponding change in the NO_y distribution for the different model initializations is shown in Figure 2. Figure 7 depicts the difference of the nitric acid distribution obtained by simple subtraction of the CLAES zonally monthly averaged HNO_3

profiles in January 1993 from the similar values in January 1992. A similar procedure is applied to the model calculated HNO_3 fields during the same period. These changes reflect a complex interplay between dynamics and chemistry of the stratosphere from January 1992 to January 1993. Below we make an attempt to separate effects of dynamics and chemistry in the HNO_3 field.

The pattern of the nitric acid change shows a strong interhemispheric difference. The area of the largest increase of HNO_3 (more than 2 ppbv) as seen by the CLAES instrument is located in the southern hemisphere between 35 and 10 mbar. Our UARS-initialized box model (bottom panel of Figure 7) captures its location and magnitude very well, albeit the area of the calculated HNO_3 change above 2 ppbv is smaller. The heterogeneous chemistry on sulfate aerosol (primarily due to $N_2O_5 + H_2O \longrightarrow 2HNO_3$) is responsible for the HNO_3 change in this area, since the change in NO_y (which could serve as an indicator of a change of stratospheric dynamics) is smaller (top panel of Figure 2) than the change in HNO_3. Also, CLAES and model calculations show positive change in the HNO_3 field almost everywhere in the southern hemisphere stratosphere, while negative change of the NO_y field is seen there above 10 mbar. In the northern mid-latitudes, positive change of HNO_3 distribution is coincident with negative change of the NO_y field. Since the opposite signs of the HNO_3 and NO_y changes at the same location imply strong repartitioning of the nitrogen species from January 1992 to January 1993 due to heterogeneous chemistry, we can conclude that the whole stratosphere has been strongly chemically perturbed during this period of time. Above 4 mbar the changes of HNO_3 (both CLAES and model) and NO_y are small.

Analysis of the change in the NO_y distribution above 20 mbar in the southern mid-latitudes shows a very weak interannual change of dynamics there from 1992 to 1993 (see Figure 2). On the other hand, the situation in the northern mid-latitudes is quite different, perhaps, due to the asymmetric QBO-like effects [*Gray and Ruth*, 1992; *Kumer et al.*, 1996a]. Changes in NO_y larger than -4 ppbv (inferred from CLAES N_2O) are present in a quite noticeable part of the stratosphere above 50 mbar in northern tropics and mid-latitudes. However, the HALOE instrument has seen somewhat smaller perturbation in the CH_4 field in this region as shown in the bottom panel of Figure 2 via the CH_4-NO_y correlation.

Model NO_y results for the N_2O and CH_4 approaches (Figure 2, middle and bottom panels) show some similarities with Figure 7. However, they also demonstrate that dynamical perturbation of the long-lived tracers such as N_2O and CH_4 (translated into NO_y change in the middle and bottom panel of Figure 2) was so strong in some locations (especially near 20 mbar at 20°N) that its fingerprint was observed in the HNO_3 field as a negative change (Figure 7) overshadow effects of heterogeneous chemistry there.

4. Discussion of the HNO_3 and NO_2 Column Data

Ground-based concurrent measurements of HNO_3 and NO_2 columns at Lauder (New Zealand, 45°S, 170°E) provide an additional opportunity to validate our model calculations and UARS measurements. Figure 8 compares monthly averaged ground based measurements (blue symbols with errorbars) of HNO_3 (top panel) and NO_2 columns at sunset (bottom panel) with UARS data and our box model calculations with the three different initializations. The CLAES daily measurements of HNO_3 at 44°S (version 8) and HALOE sunset monthly values of NO_2 between 50° and 40°S are shown by green. The CLAES instrument does not account for nitric acid below 100 mbar. To compare CLAES data with ground-based observations, we increased the partial HNO_3 column values by 0.9×10^{15} cm^{-2} as in *Kumer et al* 1996a], assuming ~70 pptv HNO_3 below 100 mbar. Following *McKenzie et al.* [1991], we assume a constant tropospheric NO_2 profile of 20 pptv in summer and 60 pptv in winter at 45° [*Logan et al.*, 1981] with sinusoidal inter-seasonal change, thus adding a value between $\sim2.8\times10^{14}$ and $\sim7.7\times10^{14}$ cm^{-2}, respectively, to the HALOE NO_2 column values. The same values of the HNO_3 and NO_2 columns below 100 mbar have been added to our box model calculations.

The ground-based NO_2 column measurements were made using a visible spectrometer based on the twilight zenith-sky technique. The NO_2 slant column amount was measured at sunrise and sunset at solar zenith angle of 90 degrees. The vertical column value was calculated assuming an air mass factor of 16.7. The absolute accuracy estimated only from the temperature dependence of the NO_2 absorption cross-section was +18 ± 5 % (overestimate), because the 20°C values were used for the analyses. Uncertainty in the air mass factor was estimated to be ± 12 %. Other sources of the systematic error are described in *Koike et al.* [1998]. Vertical column HNO_3

amount was measured using Fourier transform infrared spectrometer. The absolute accuracy estimated from uncertainties in the HNO_3 absorption line parameter and vertical HNO_3 profile was $\pm$ 13 % [*Jones et al.*, 1994].

The ground-based and CLAES measurements of the HNO_3 agree well from January 1992 to May 1993, while the box-model calculations are consistent with the measurements after August 1992 for all initializations. The CH_4- and N_2O-initialized box model overestimates the vertical HNO_3 amount in the first half of 1992 due to overestimate of the NO_y content below 30 mbar inferred from the N_2O and CH_4 fields and shown in Figure 1. Our UARS initialization can provide the column value only during the first ($\approx$January) and third ($\approx$March) yaw cycles in 1993 (shown by black symbol), primarily, because of the missing HALOE NO_2 measurements at the lowermost levels (100 and 68 mbar) affected by the Pinatubo cloud. Both ground-based and CLAES measurements capture a noticeable increase of the HNO_3 column in summer 1992 at the top of its seasonal cycle due to enhanced NO_x conversion on Pinatubo aerosol. Unfortunately, our box model could not be initialized during May-July 1992 due to missing HALOE measurements at this latitude.

Analysis of the NO_2 column data (bottom panel) demonstrates a recovery of NO_2 after the Pinatubo eruption and good agreement between ground-based and HALOE sunset measurements. Our box model calculations, as could be anticipated from our section 3 and previous comparisons [*Koike et al.*, 1994; *Rosenfeld et al.*, 1997], considerably underestimates the NO_2 column up to 50% with the ground-based measurements during the whole period of time investigated. As we show in Figure 6, the reason of this discrepancy is mainly due to the model underestimate of the NO_2 content between 30 and 6 mbar. Assuming 50% NO_2 underestimation in the model in the 20-35 km altitude range (which can contributes $\sim$75% of the total NO_2 column [*McKenzie et al*, 1991; their Figure 8] in summer, we increase our model column values by $\sim$38%, making them much closer to the ground-based and HALOE measurements. The new version 18 of HALOE data is in better agreement with the ground-based measurements than the version 17 results [*Gordley et al.*, 1996].

Results for the sunrise NO_2 column show a very similar pattern with lower absolute values by a factor of $\sim$1.6 and are not shown here. Satisfactory agreement of the HNO_3 column

values and disagreement of NO_2 column values between model calculations and measurements indicates problems in the model's ability to reproduce proper partitioning between NO_x and HNO_3 rather than an incorrect initialization of NO_y. A similar problem was obtained in the AER 2-D model calculations for the post-Pinatubo conditions (not shown here). Also, our box model showed very similar results as the GSFC 3-D model and both models underpredict the NO content in the stratosphere during analysis of the balloon measurements in September 1994 [*Kondo et al.*, 1998]. As we mentioned above, several other models with state-of-the-art heterogeneous chemistry and updated photochemical kinetics underestimated the NO_x content in the stratosphere [e.g. *Lary et al.*, 1996; *Morris et al.*, 1997; *Sen et al.*, 1998].

Figure 9 shows a comparison of the ground-based (Moshiri station, Japan, 44°N), HALOE and model values of the NO_2 column at 45°N which depicts similar problems outlined in our discussion for 45°S. The HALOE v.18 NO_2 column agrees well with the ground-based measurements. Our model calculations are smaller than the ground-based measurements by about 50% through the whole year. A similar pattern is obtained for sunrise conditions. The reasons for these discrepances are outlined above.

5. Conclusions

We have presented analyses of the UARS measurements (HALOE and CLAES) using the AER diurnal steady-state box model from January 1992 to September 1994. It was shown that use of zonal yaw-averaged UARS measurements, which avoid high uncertainties of the UARS individual profiles and considerably reduce computer time for analysis, captures the principal features of the nitrogen species partitioning in the global post-Pinatubo stratosphere.

The AER diurnal steady-state photochemical stratospheric model, with proper constraints from the UARS measurements, can be rather successfully applied for analysis of this data set. We discussed three possibilities listed in Table 1 to initialize the box model from the available set of UARS measurements. Each of them has particular advantages and disadvantages. Our analysis shows that the UARS and N_2O approaches can provide reasonable agreement in the NO_x/NO_y ratio between model calculations and UARS data (especially in the upper stratosphere). However, they are limited by the CLAES operation time (until May 1993). The CH_4

approach has a larger temporal coverage, but is has several outlined weaknesses, like overestimation of NO_y above 10 mbar in the tropics.

In general, our results show that the model and the approach used provide good agreement with the UARS data below 30 mbar, thus supporting our current parameterization of the heterogeneous reactions on sulfate aerosol. Our analysis, concentrated at 45°S and 45°N, revealed a seasonally modulated gradual increase of the NO_x/NO_y ratio after the Pinatubo eruption in the lower and middle stratosphere, consistent with the UARS measurements. Our state-of-the-art module of heterogeneous chemistry on sulfate aerosol reproduces the vertical profiles of NO, NO_2, and HNO_3 along with the temporal evolution of the latitudinal-altitudinal distribution of these species.

Among clear discrepances between model results and UARS measurements, we emphasize a clear underestimation of the NO_2 content at the 30-7 mbar levels (particularly evident in the summer hemisphere) in our box model. Since the aerosol loading is very low at these altitudes, it signals possible problems in gas-phase chemistry or photolytic processes. This problem has been noted in previous studies [e.g. *Considine et al.*, 1992; *Morris et al.*, 1997; *Sen et al*, 1998], however, there is no clear understanding yet of why it occurs. Analysis of the NO_2 column measurements show that the ground-based (at Lauder, New Zealand, 45°S and Moshiri, Japan, 44°N) and HALOE v.18 data are consistent within the range of their uncertainties, while the model calculations underestimate the NO_2 amount by up to 50% during the period and latitudes considered. Further analysis is urgently needed to understand the reason for the model underestimation of NO_2 at these altitudes (~24-34 km) and its consequencies for global 2-D (3-D) model predictions.

Acknowledgements

The work at AER, Inc. is supported by the NASA UARS Guest Investigator Program (contract NAS5-32844).

References

Bekki, S. and J.A. Pyle, A two-dimensional modeling study of the volcanic eruption of Mount Pinatubo, *J. Geophys. Res.*, *99*, 18,862-18,869, 1994.

Bekki, S., On the possible role of aircraft generated soot in the middle latitude ozone depletion, *J.*

Geophys. Res., 102, 10,751-10,758, 1997.

Boville, B.A., J.R. Holton, and P.W. Mote, Simulation of the Pinatubo aerosol cloud in GCM, *Geophys. Res. Lett., 18*, 2281-2284, 1991.

Brasseur, G.P. and C. Granier, Mount Pinatubo aerosols, chlorofluorocarbons, and ozone depletion, *Science, 257,* 1239-1242, 1992.

Considine, D.B., A.R. Douglass, and R.S. Stolarski, Heterogeneous conversion of N_2O_5 to HNO_3 on background stratospheric aerosols: comparisons of model results with data, *Geophys. Res. Lett., 19*, 397-400, 1992.

Danilin, M.Y., and J.C. McConnell, Stratospheric effects of bromine activation on/in sulfate aerosol, *J. Geophys. Res., 100,* 11,237-11,243, 1995.

David, S.J., F.J. Murcray, A. Goldman, C.P. Rinsland, and D.G. Murcray, The effect of the Mt. Pinatubo aerosol on the HNO_3 column over Mauna Loa, Hawaii, *Geophys. Res. Lett., 21*, 1003-1006, 1994.

DeMore, W.B. et al, Chemical kinetics and photochemical data for use in stratospheric modeling. Evaluation number 12. *JPL-Publication 97-4,* 1997.

Dessler, A.E., et al., Correlated observations of HCl and $ClONO_2$ from UARS and implications for stratospheric chlorine partitioning, *Geophys. Res. Lett., 22*, 1721-1724, 1995.

Dessler, A.E. et al., A test of the partitioning between ClO and $ClONO_2$ using simultaneous UARS measurements of ClO, NO_2, and $ClONO_2$, *J. Geophys. Res. 101*, 12,515-12,521, 1996.

Dessler, A.E., et al., Selected science highlights from the first 5 years of the UARS program, *Rev. Geophys., 36*, 183-210, 1998.

Donahue, N.M., M.K. Dubey, R. Mohrschladt, K.L. Demerjian, and J.G. Anderson, High-pressure flow study of the reactions OH + $NO_x \longrightarrow HONO_x$: Errors in the falloff region, *J. Geophys. Res., 102*, 6159-6168, 1997.

Fairbrother, D.H., D.J.D. Sullivan, and H.S. Johnston, Global thermodynamic atmospheric modeling: Search for new heterogeneous reactions, *J. Phys. Chem., 101*, 7350-7358, 1997.

Fahey, D.W. et al., A diagnostic for denitrification in the winter polar stratosphere, *Nature, 345*, 698-702, 1990.

Fahey, D.W. et al., In situ measurements constraining the role of sulfate aerosols in mid-latitude

ozone depletion, *Nature, 363*, 509-514, 1993.

Gao, R.S. et al., Partitioning of the reactive nitrogen reservoir in the lower stratosphere of the southern hemisphere: Observations and modeling, *J. Geophys. Res., 102*, 3935-3949, 1997.

Gille, J.C., et al., Accuracy and precision of the nitric acid concentrations determined by the limb infrared monitor of the stratosphere experiment on Nimbus 7, *J. Geophys. Res., 89*, 5179-5190, 1984.

Gordley, L.L., et al., Validation of nitric oxide and nitrogen dioxide measurements made by HALOE for UARS platform, *J. Geophys. Res., 101,* 10,241-10,266, 1996.

Gray, L.J. and S. Ruth, The interannual variability of trace gases in the stratosphere: A comparative study of the LIMS and UARS measurement periods, *Geophys. Res. Lett., 19*, 673-676, 1992.

Hanson, D.R., A. R. Ravishankara, and E.R. Lovejoy, Reaction of $BrONO_2$ with H_2O on submicron sulfuric acid aerosol and the implications for the lower stratosphere, *J. Geophys. Res., 101,* 9063-9069, 1996.

Hu, W., J.M. Rodriguez, M.K.W. Ko, M.Y.Danilin, D.K. Weisenstein, J.M. Russell III, J.B. Kumer, and G.K. Yue, Ozone balance in the stratosphere as seen by the UARS, *J. Geophys. Res., to be submitted*, 1998.

Iraci, L.T., and M.A. Tolbert, Heterogeneous interaction of formaldehyde with cold sulfuric acid, *J. Geophys. Res., 102,* 16,099-16,107, 1997.

Jackman, C.H., et al., An intercomparison of nitrogen-containing species in Nimbus 7 LIMS and SAMS data, *J. Geophys. Res., 92*, 995-1008, 1987.

Johnston, P.V. et al., Observations of depleted stratospheric NO_2 following the Pinatubo volcanic eruption, *Geophys. Res. Lett., 19*, 211-213, 1992.

Jones, N.B., M. Koike, W.A. Matthews, and B.M. McNamara, Southern hemisphere mid-latitude seasonal cycle in total column nitric acid, *Geophys. Res. Lett., 21*, 593-596, 1994.

Jucks, K.W., D.G. Johnson, K.V. Chance, W.A. Traub, R.J. Salawitch, and R.A. Stachnik, Ozone production and loss rate measurements in the middle stratosphere, *J. Geophys. Res., 101*, 28,785-28,792, 1996.

Kawa, S.R., et al., Interpretation of NO_x/NO_y observations from AASE-II using a model of chemistry along trajectories, *Geophys. Res. Lett., 20*, 2507-2510, 1993.

Kaye, J.A. and T.L. Miller, The ATLAS series of Shuttle missions, *Geophys. Res. Lett., 23*, 2285-2288, 1996.

Keim, E.R., et al., Measurements of the NO_y-N_2O correlation in the lower stratosphere: Latitudinal and seasonal changes and model comparisons, *J. Geophys. Res., 102,* 13,193-13,212, 1997.

Kinnison, D.E. et al., The chemical and radiative effects of the Mt. Pinatubo eruption, *J. Geophys. Res., 99*, 22,705-22,731, 1994.

Koike, M. et al., Decrease of stratospheric NO_2 at 44°N caused by Pinatubo volcanic aerosols, *Geophys. Res. Lett., 20*, 1975-1978, 1993.

Koike, M. et al., Impact of Pinatubo aerosols on the partitioning between NO_2 and HNO_3, *Geophys. Res. Lett., 21*, 597-600, 1994.

Koike, M., Y. Kondo, W.A. Matthews, P.V. Johnston, H. Nakajima, A. Kawaguchi, H. Nakane, I. Murata, A. Budiyno, M. Kanada, and N. Toriyama, Assessment of the uncertainties in the NO_2 and O_3 measurements by visible spectrometers, *J. Atmos. Chem., in press,* 1998.

Kondo, Y., et al., NO_y correlation with N_2O and CH_4 in the mid-latitude stratosphere, *Geophys. Res. Lett., 23*, 2369-2372, 1996.

Kondo, Y., et al., Effect of Pinatubo aerosol on stratospheric NO. *J. Geophys. Res., 102*, 1205-1213, 1997.

Kondo, Y., et al., Partitioning of reactive nitrogen in the midlatitude lower stratosphere, *J. Geophys. Res., to be submitted*, 1998.

Kumer, J.B., et al., Comparison of correlative data with HNO_3 version 7 from the CLAES instrument deployed on the NASA UARS, *J. Geophys. Res., 101*, 9621-9656, 1996a.

Kumer, J.B., et al., Comparison of CLAES preliminary N_2O_5 data with correlative data and a model, *J. Geophys. Res., 101*, 9657-9677, 1996b.

Lambert, A., et al., Global evolution of the Mt. Pinatubo volcanic aerosols observed in the infrared limb-sounding instruments CLAES and ISAMS on the UARS *J. Geophys. Res., 102*, 1495-1512, 1997.

Lary, D.J., M.P. Chipperfiled, R. Toumi, and L. Lenton, Heterogeneous atmospheric bromine chemistry, *J. Geophys. Res., 101*, 1489-1504, 1996.

Lary, D.J., R. Toumi, A.M. Lee, M.J. Newchurch, M. Pirre, and J.B. Renard, Carbon aerosols and

atmospheric photochemistry, *J. Geophys. Res., 102*, 3671-3682, 1997.

Loewenstein, M. et al., New observations of the NO_y/N_2O correlation in the lower stratosphere, *Geophys. Res. Lett., 20*, 2531-2534, 1993.

Logan, J.A., M.J. Prather, S.C. Wofsy, and M.B. McElroy, Tropospheric chemistry: A global perspective, *J. Geophys. Res., 86*, 7210-7254, 1981.

McKenzie, R.L., P.V. Johnston, C.T. McElroy, J.B. Kerr, and S.Solomon, Altitude distributions of stratospheric constituents from ground-based measurements at twilight, *J. Geophys. Res., 96,* 15,499-15,511, 1991.

Michelsen, H.A., G.L. Manney, M.R. Gunson, and R. Zander, Correlations of stratospheric NO_y, O_3, N_2O, and CH_4 derived from ATMOS measurements, *J. Geophys. Res., in press*, 1998.

Morris, G.A. et al., Trajectory mapping of UARS data, *J. Geophys. Res., 100*, 16,491-16,505, 1995.

Morris, G.A., et al., Nitrogen partitioning in the middle stratosphere as observed by UARS, *J. Geophys. Res., 102,* 8955-8965, 1997.

Nevison, C.D., S. Solomon, and R.R. Garcia, Model overestimates of NO_y in the upper stratosphere, *Geophys. Res. Lett., 24*, 803-806, 1997.

Nolholt, J., The Moon as a light source for FTIR measurements of stratospheric trace gases during the polar night: Application for HNO_3 in the Arctic, *J. Geophys. Res., 99*, 3607-3614, 1994.

Osterman, G.B. et al., Balloon-borne measurements of stratospheric radicals and their precursors: Implications for the production and loss of ozone, *Geophys. Res. Lett, 24*, 1107-1110, 1997.

Park, J.H., et al., Validation of HALOE CH_4 measurements from the UARS, *J. Geophys. Res., 101*, 10183-10203, 1996.

Pitari, G. and V. Rizi, An estimate of the chemical and radiative perturbation of stratospheric ozone following the eruption of Mt. Pinatubo, *J. Atmos. Sci., 50*, 3260-3276, 1993.

Prather, M.J. and E.E. Remsberg (eds), The atmospheric effects of stratospheric aircraft: report of the 1992 models and measurements workshop, *NASA Ref. Publ. 1292, vol.III*, Chapter H, 1993.

Preston, K.E., R.L. Jones, and H.K. Roscoe, Retrieval of NO_2 vertical profiles from ground-based UV-visible measurements: Method and validation, *J. Geophys. Res., 102*, 19,089-19,098, 1997.

Reber, C.A., et al., The upper atmosphere research satellite mission, *J. Geophys. Res., 98*, 10,643-

10,647, 1993.

Renard, J-B., et al., Vertical distribution of night-time stratospheric NO_2 from balloon measurements: comparison with models, *Geophys. Res. Lett., 24*, 73-76, 1997.

Renard, J-B., et al., Nocturnal vertical distribution of stratospheric O_3, NO_2, and NO_3 from balloon measurements, *J. Geophys. Res., 101*, 28,793-28,804, 1996.

Ridley, B.A., et al., Stratospheric add nitrogen: measurements of HNO_3, NO, NO_2, and O_3 near 54°N in winter, *J. Geophys. Res., 89*, 4797-4820, 1984.

Ridley, B.A., et al., Seasonal differences in the vertical distributions of NO, NO_2, and O_3 near 50°N, *J. Geophys. Res., 92*, 11,919-11,929, 1987.

Rinsland, C.P. et al., Heterogeneous conversion of N_2O_5 to HNO_3 in the post-Mt. Pinatubo eruption stratosphere, *J. Geophys. Res., 99*, 8213-8219, 1994.

Roche, A.E. et al., Validation of CH_4 and N_2O measurements by the CLAES instrument on the UARS, *J. Geophys. Res., 101*, 9679-9710, 1996.

Rodriguez, J.M., M.K.W. Ko, and N.D. Sze, Role of heterogeneous conversion of N_2O_5 on sulfate aerosol in global ozone loss, *Nature, 352,* 134-137, 1991.

Rodriguez, J.M. et al., Ozone response to enhanced heterogeneous processing after the eruption of Mt. Pinatubo, *Geophys. Res. Lett., 21*, 209-212, 1994.

Rogaski, C.A., D.M. Golden, and L.R. Williams, Reactive uptake and hydration experiments on amorphous carbon, *Geophys. Res. Lett., 34*, 381-384, 1997.

Rood, R.B., A.R. Douglass, J.A. Kaye, and D.B. Considine, Characteristics of wintertime and autumn nitric acid chemistry as defined by LIMS data, *J. Geophys. Res., 98*, 18,533-18,545, 1993.

Rosenfeld, J.E., et al., Stratospheric effects of Mount Pinatubo aerosol studied with a coupled 2-D model, *J. Geophys. Res., 102*, 3649-3670, 1997.

Russell, J.M. III, et al., The variability of stratospheric and mesospheric NO_2 in the polar winter night observed by LIMS, *J. Geophys. Res., 89*, 7267-7275, 1984.

Sen, B. et al., Measurements of reactive nitrogen in the stratosphere, *J. Geophys. Res., 103*, 3571-3585, 1998.

Slusser, J.R., D.J. Fish, E.K. Strong, R.L. Jones, H.K. Roscoe, and A. Sarkissian, Five years of

NO_2 vertical column measurements at Faraday (65°S): Evidence for the hydrolysis of $BrONO_2$ on Pinatubo aerosol, *J. Geophys. Res., 102*, 12,987-12,993, 1997.

Slusser, J., et al., High-latitude stratospheric NO_2 and HNO_3 over Fairbanks (65°N) 1992-1994, *J. Geophys. Res., 103*, 1549-1554, 1998.

Solomon, S., et al., The role of aerosol variations in anthropogenic ozone depletion at northern midlatitudes, *J. Geophys. Res., 101*, 6713-6727, 1996.

Thomason, L.W., L.R. Poole, and T. Deshler, A global climatology of stratospheric aerosol surface area density deduced from SAGE II measurements: 1984-1994, *J. Geophys. Res., 102*, 8967-8976, 1997.

Tie, X.X. et al., Two-dimensional simulation of Pinatubo aerosol and its effect on stratospheric ozone, *J. Geophys. Res., 99,* 20,545-20,562, 1994.

Van Roozendael, M., et al., Ground-based observations of stratospheric NO_2 at high and mid-latitudes in Europe after the Mt Pinatubo eruption, *J. Geophys. Res., 102*, 19,171-19,176, 1997.

Wamsley, P.R., et al., Distribution of halon-1211 in the upper troposphere and lower stratosphere and the 1994 total bromine budget, *J. Geophys. Res., 103*, 1513-1526, 1998.

Weisenstein, D.K., et al., A two dimensional model of sulfur species and aerosols, *J. Geophys. Res, 102,* 13,019-13,035, 1997.

Woodbridge, E.L., et al., Estimates of total organic and inorganic chlorine in the lower stratosphere from in situ and flask measurements during AASE II, *J. Geophys. Res., 100*, 3057-3064, 1995.

Yue, G.K., L.R. Poole, P.-H. Wang, and E.W. Chiou, Stratospheric aerosol acidity, density, and refractive index deduced from SAGE II and NMC temperature data, *J. Geophys. Res., 99*, 3727-3738, 1994.

Zipf, E.C. and S.S. Prasad, Evidence for new sources of NO_x in the lower atmosphere, *Science, 279*, 211-213, 1998.

Table 1. Heterogeneous reactions on sulfate aerosol included in the model. The reaction probabilities are taken from *DeMore et al.* [1997], except the $BrONO_2 + H_2O$ reaction (see text).

$N_2O_5 + H_2O$	$\longrightarrow$	$HNO_3 + HNO_3$
$BrONO_2 + H_2O$	$\longrightarrow$	$HOBr + HNO_3$
$ClONO_2 + H_2O$	$\longrightarrow$	$HOCl + HNO_3$
$ClONO_2 + HCl$	$\longrightarrow$	$Cl_2 + HNO_3$
$HOCl + HCl$	$\longrightarrow$	$Cl_2 + H_2O$
$HOBr + HCl$	$\longrightarrow$	$BrCl + H_2O$

Table 2. Initialization methods for NO_y, Cl_y, and Br_y employed in this study, using the UARS data.

SPECIES		APPROACH	
	UARS	N_2O^{CLAES}	CH_4^{HALOE}
NO_y below 7 mbar	NO_y^U	$f_1(N_2O^c)$	$f_4(CH_4)$
NO_y above 7 mbar	NO_y^U	NO_y^U	$f_4(CH_4)$
Cl_y	$f_2(N_2O^c)$	$f_2(N_2O^c)$	$f_2(N_2O^*)$
Br_y	$f_3(N_2O^c)$	$f_3(N_2O^c)$	$f_3(N_2O^*)$

$NO_y^U = <NO^U> + <NO_2^U> + <HNO_3^U> + <ClONO_2^U>$, N_2O^c is the monthly CLAES N_2O data, N_2O^* is the N_2O value from the CH_4-N_2O correlation (see text); function $f_1(N_2O)$ is defined by *Keim et al* [1997] and by *Loewenstein et al.* [1993] in the southern and northern hemisphere, respectively; functions $f_2(N_2O)$, $f_3(N_2O)$, and $f_4(CH_4)$ are defined according to *Woodbridge et al.* [1995], *R.J. Salawitch*, and *Michelsen et al.* [1998], respectively (see text).

Figure Captions

Figure 1. Difference (in %) between model NO_x/NO_y calculated for monthly zonally averaged UARS data and for daily UARS data averaged over month and longitude. The CH_4 approach to initialize model runs has been used. A gap between 25°S and 5°N is due to the geometry

of HALOE measurements in February 1993 (sunrise and sunset measurements in the southern and northern hemisphere, respectively).

Figure 2. Distribution of NO_y (in ppbv, top panel) in January 1993 using the UARS initialization (see Table 1). The middle and bottom panels show the difference between NO_y^{UARS} and NO_y as inferred from the correlations with CLAES zonal monthly averaged $<N_2O^c>$ and HALOE $<CH_4>$, respectively (see text for details).

Figure 3. Change of NO_y between January 1992 and January 1993 inferred from the different methods of NO_y initialization according to: the UARS approach (top panel); the N_2O approach (middle panel), and the CH_4 approach (bottom panel).

Figure 4. Temporal evolution of the sunset NO_x/NO_y ratio from January 1992 to September 1994 at 45°S (left column) and 45°N (right column) at the 68, 46, 32, and 22 mbar levels. Green, cyan, and blue symbols with errorbars correspond to the UARS data with NO_y according to the CH_4, UARS, and N_2O initializations, respectively; red crosses to box model calculations. The N_2O and UARS approaches can provide NO_y data only until May 1993 because of the CLAES lifetime. The black lines show behavior of aerosol surface area density (right vertical axis, in $\mu m^2/cm^3$).

Figure 5. Latitudinal dependence of the sunset NO_x/NO_y ratio in January 1993 at the levels shown between 68.2 and 4.6 mbar. Model results with and without heterogeneous reactions on sulfate aerosol are shown by red and black lines, respectively. Model results with heterogeneous chemistry and with reduced by 25% reaction rate of $OH + NO_2 + M \longrightarrow HNO_3 + M$ are shown by grey lines. The UARS values are shown by symbols for the three methods of NO_y initialization: cyan for NO_y(UARS), green for $NO_y(CH_4)$, and blue for $NO_y(N_2O)$.

Figure 6. Vertical profiles of NO (blue), NO_2 (cyan), and HNO_3 (red) in January 1993 at 45°S (top panel) and 35°N (bottom panel) at sunset. UARS data are shown by symbols with errorbars, model results are shown by solid (with heterogeneous reactions) and dashed (without heterogeneous reactions) lines according to the UARS initialization.

Figure 7. Change of the zonally averaged HNO_3 distribution (in ppbv) from January 1992 to January 1993 according to the CLAES measurements (top panel) and model calculations for the UARS initialization (bottom panel).

Figure 8. HNO_3 (top panel) and sunset NO_2 (bottom panel) columns at 45°S between January 1992 and January 1995. Blue symbols show ground-based measurements in Lauder (New Zealand); red, pink and black symbols- box model results for the CH_4, N_2O and UARS initializations, respectively. Green curves in the top panel depict daily HNO_3 column values at 44°S according to the CLAES instrument (version 8). Green symbols in the bottom panel show monthly- zonally averaged HALOE (v.18) values of the sunset NO_2 column. The box model and UARS data are increased by partial HNO_3 and NO_2 columns below 100 mbar (see text).

Figure 9. Comparison of the NO_2 column (in $10^{15}cm^{-2}$) at sunset according to the ground-based measurements at Moshiri (44°N, blue), our box model calculations (red - CH_4 approach, pink crosses- N_2O approach, and black- UARS approach), and the HALOE monthly-zonally averaged data (green) from January 1992 to January 1995. The sunrise measurements (not shown) depict similar pattern with $\sim$ 1.6 times smaller values.

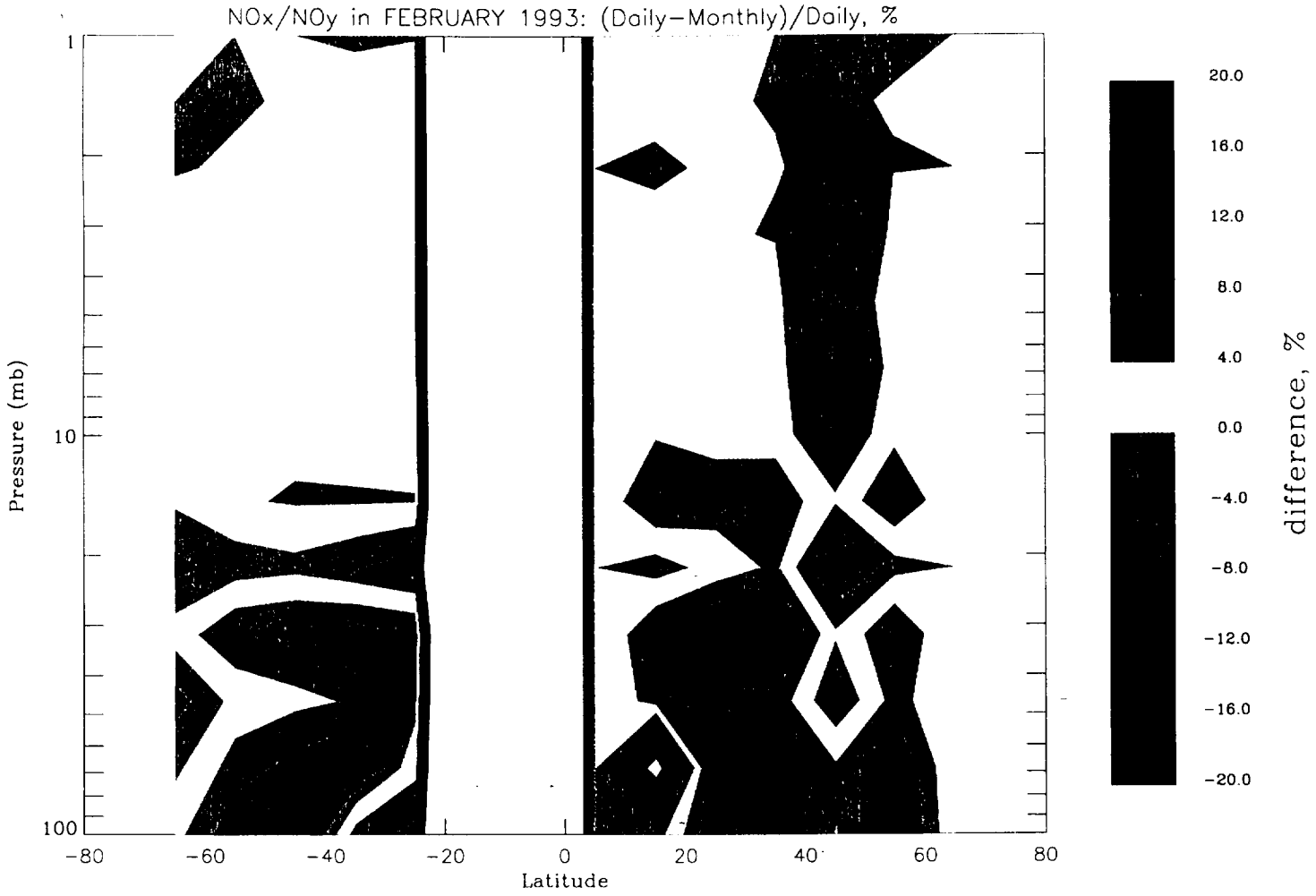
NOx/NOy in FEBRUARY 1993: (Daily−Monthly)/Daily, %
Pressure (mb)
1
10
100
−80
−60
−40
−20
0
20
40
60
80
Latitude
20.0
16.0
12.0
8.0
4.0
0.0
−4.0
−8.0
−12.0
−16.0
−20.0
difference, %

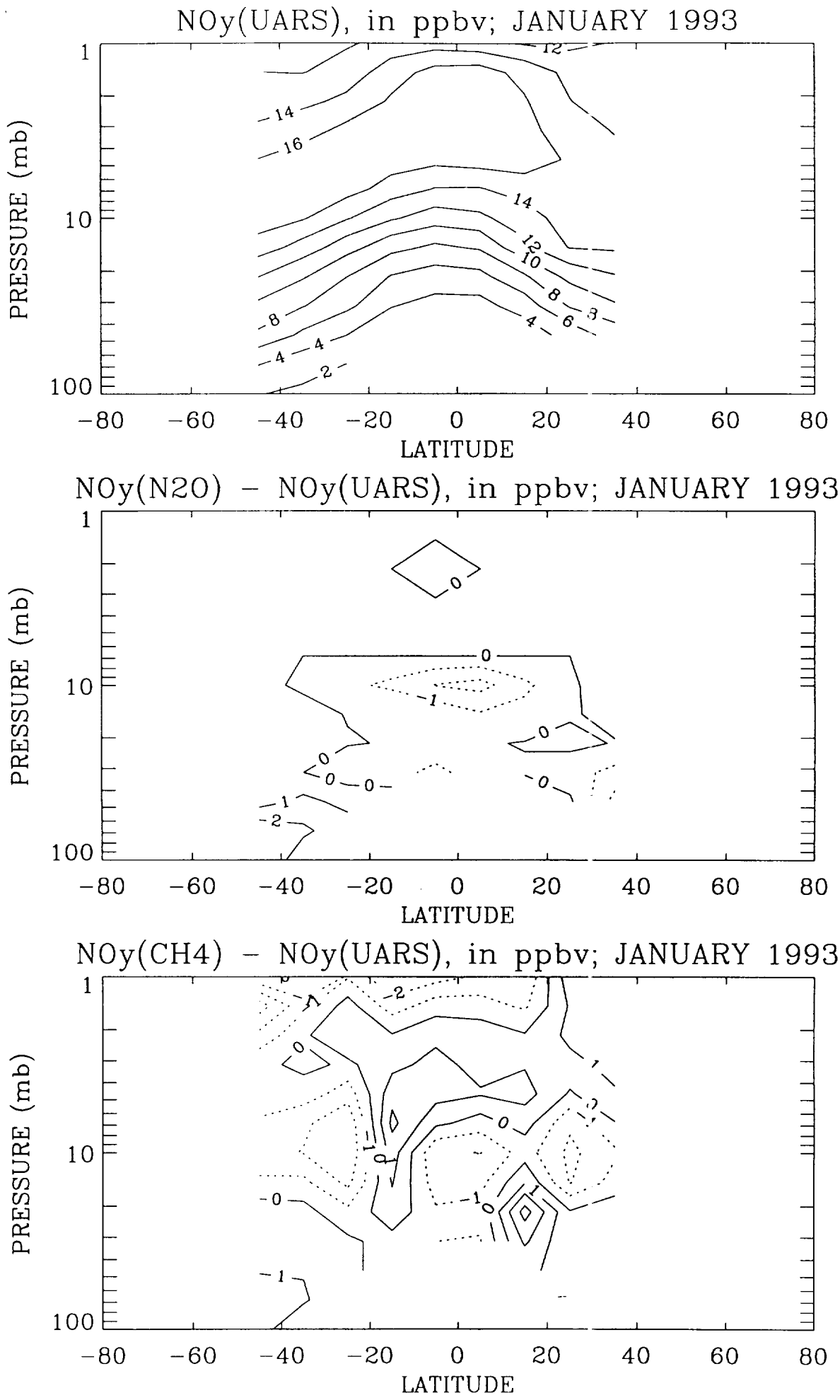
NOy(UARS), in ppbv; JANUARY 1993
PRESSURE (mb)
1
10
100
LATITUDE
-80 -60 -40 -20 0 20 40 60 80
NOy(N2O) - NOy(UARS), in ppbv; JANUARY 1993
PRESSURE (mb)
1
10
100
LATITUDE
-80 -60 -40 -20 0 20 40 60 80
NOy(CH4) - NOy(UARS), in ppbv; JANUARY 1993
PRESSURE (mb)
1
10
100
LATITUDE
-80 -60 -40 -20 0 20 40 60 80

Figure 2.

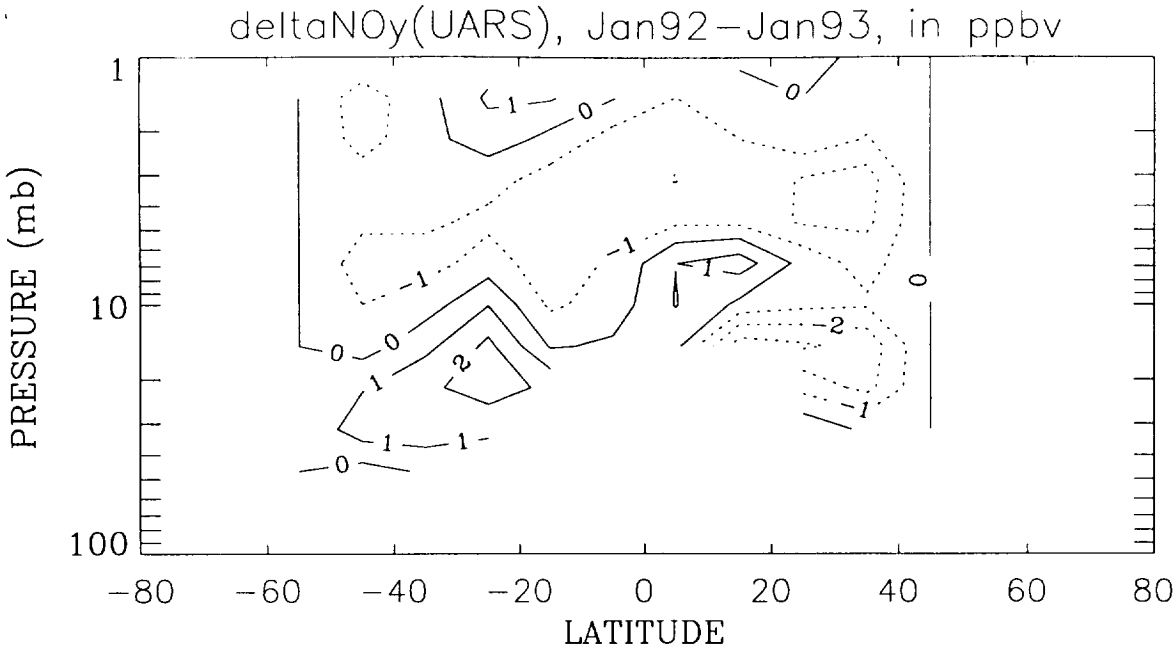
deltaNOy(UARS), Jan92–Jan93, in ppbv
PRESSURE (mb)
1
10
100
−80 −60 −40 −20 0 20 40 60 80
LATITUDE

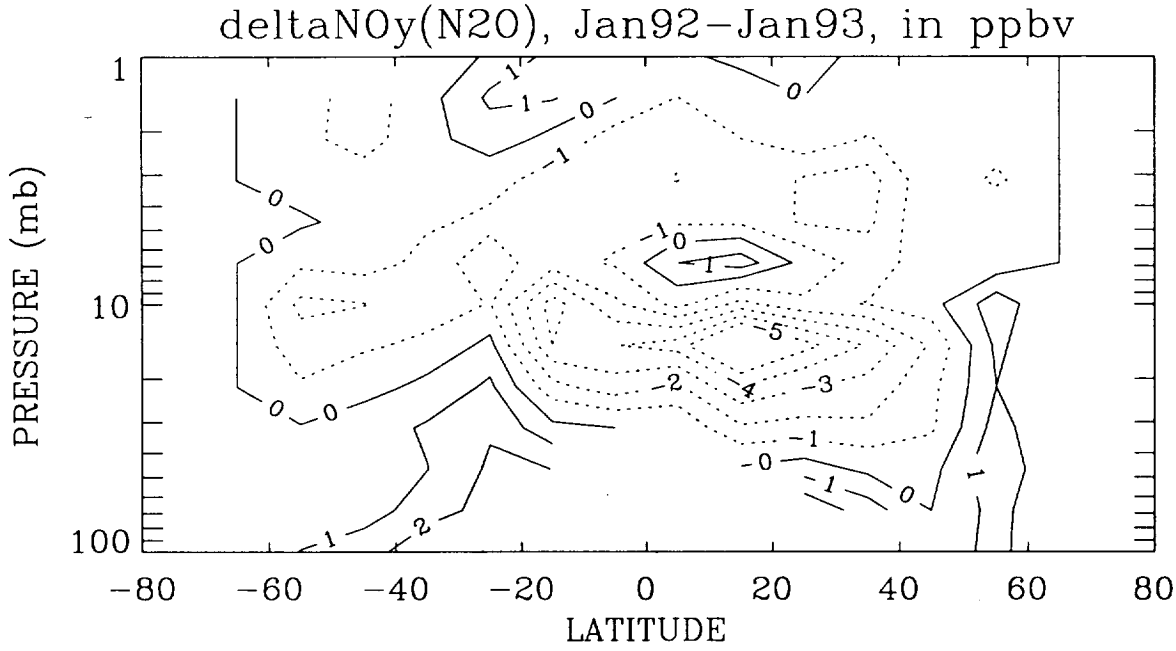
deltaNOy(N2O), Jan92–Jan93, in ppbv
PRESSURE (mb)
1
10
100
−80 −60 −40 −20 0 20 40 60 80
LATITUDE

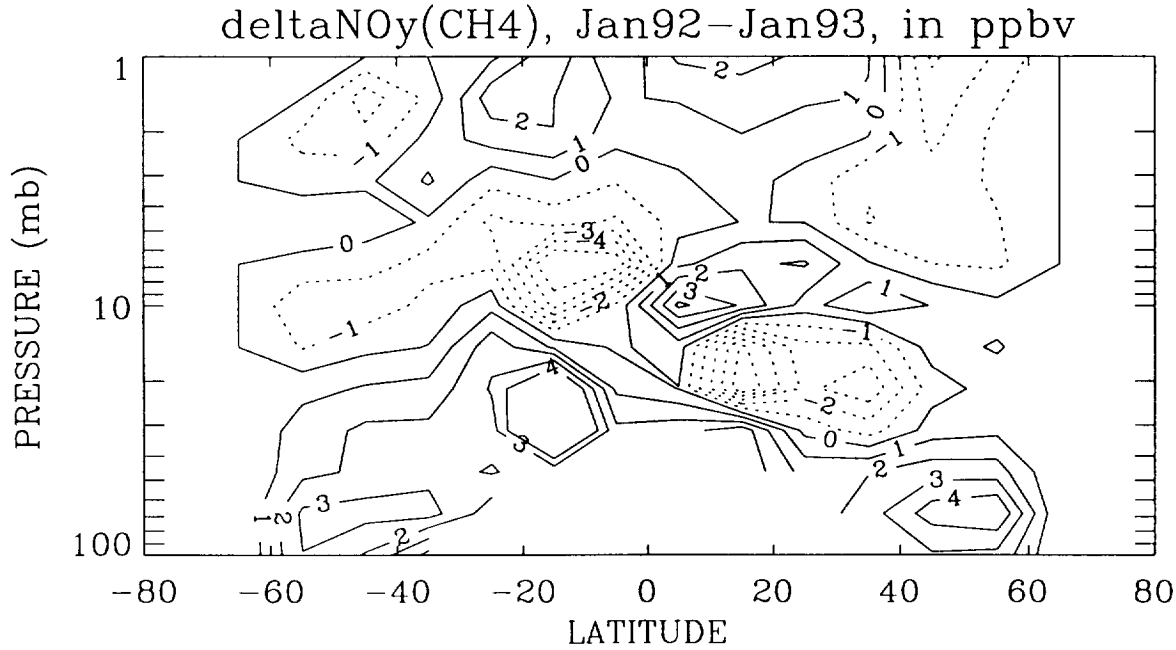
deltaNOy(CH4), Jan92–Jan93, in ppbv
PRESSURE (mb)
1
10
100
−80 −60 −40 −20 0 20 40 60 80
LATITUDE

Figure 3.

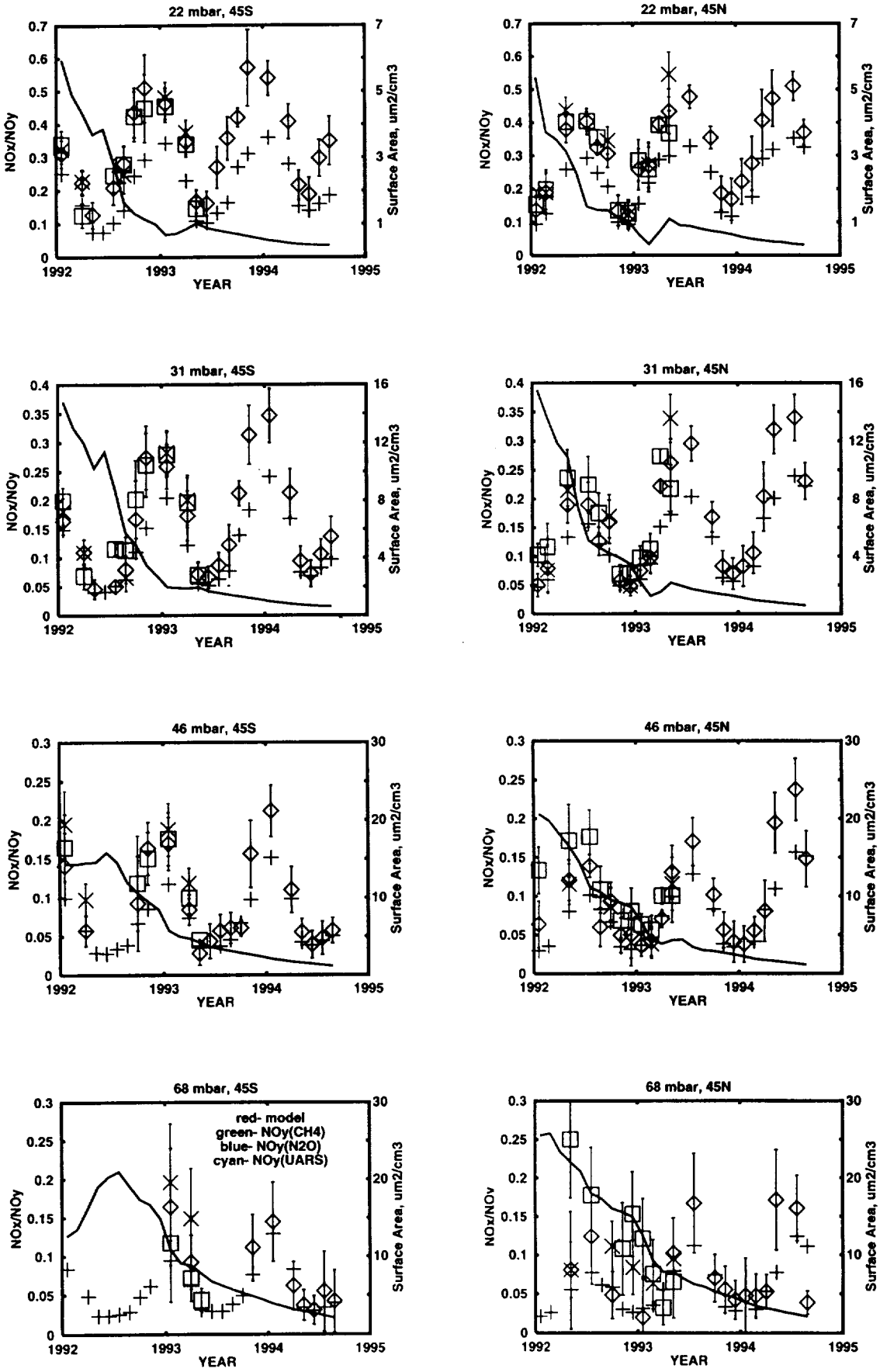
22 mbar, 45S
22 mbar, 45N
31 mbar, 45S
31 mbar, 45N
46 mbar, 45S
46 mbar, 45N
68 mbar, 45S
68 mbar, 45N
NOx/NOy
Surface Area, um2/cm3
YEAR
1992
1993
1994
1995
red- model
green- NOy(CH4)
blue- NOy(N2O)
cyan- NOy(UARS)

FIGURE 4.

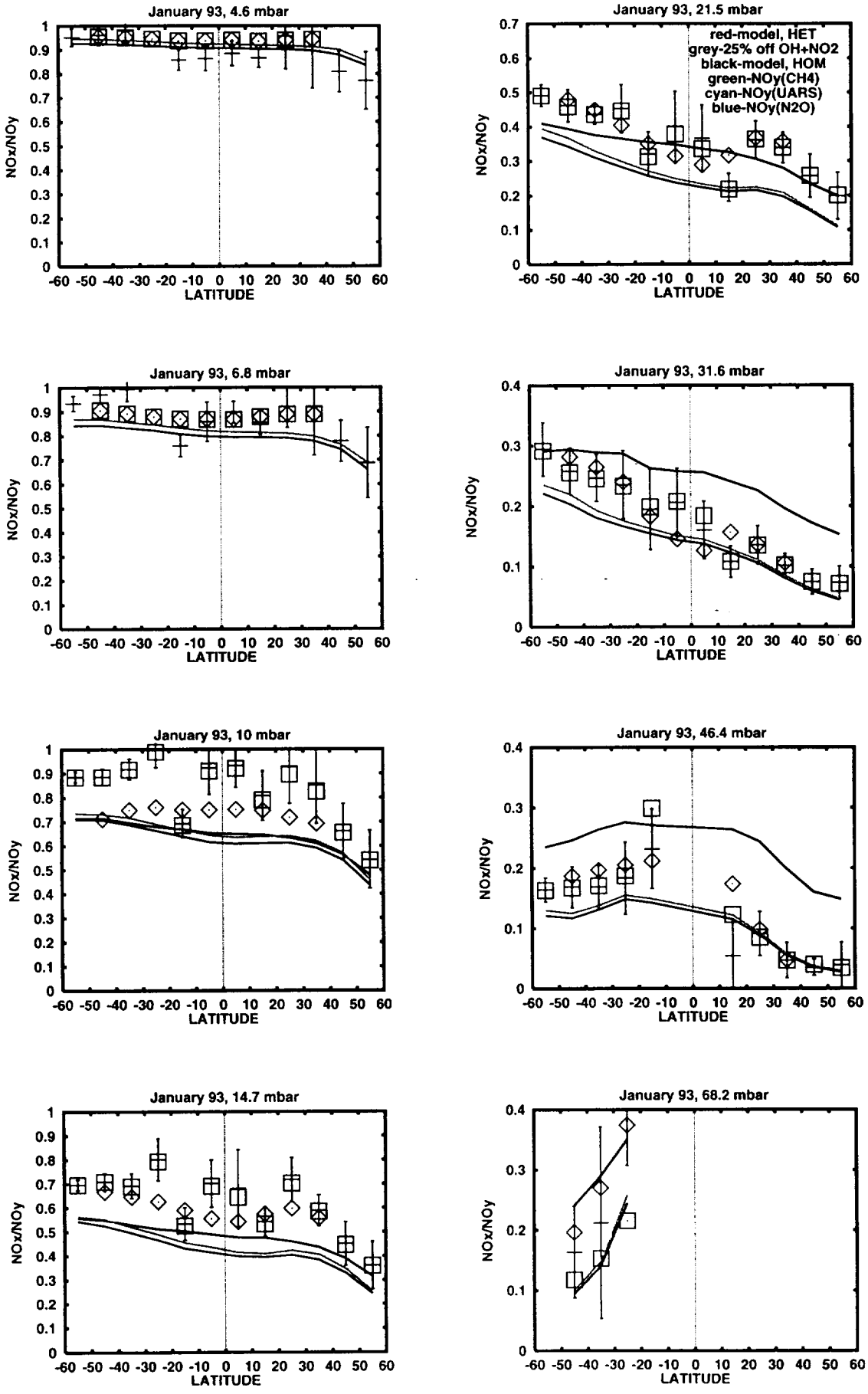
January 93, 4.6 mbar
January 93, 21.5 mbar
red-model, HET
grey-25% off OH+NO2
black-model, HOM
green-NOy(CH4)
cyan-NOy(UARS)
blue-NOy(N2O)
January 93, 6.8 mbar
January 93, 31.6 mbar
January 93, 10 mbar
January 93, 46.4 mbar
January 93, 14.7 mbar
January 93, 68.2 mbar
NOx/NOy
LATITUDE

FIGURE 5.

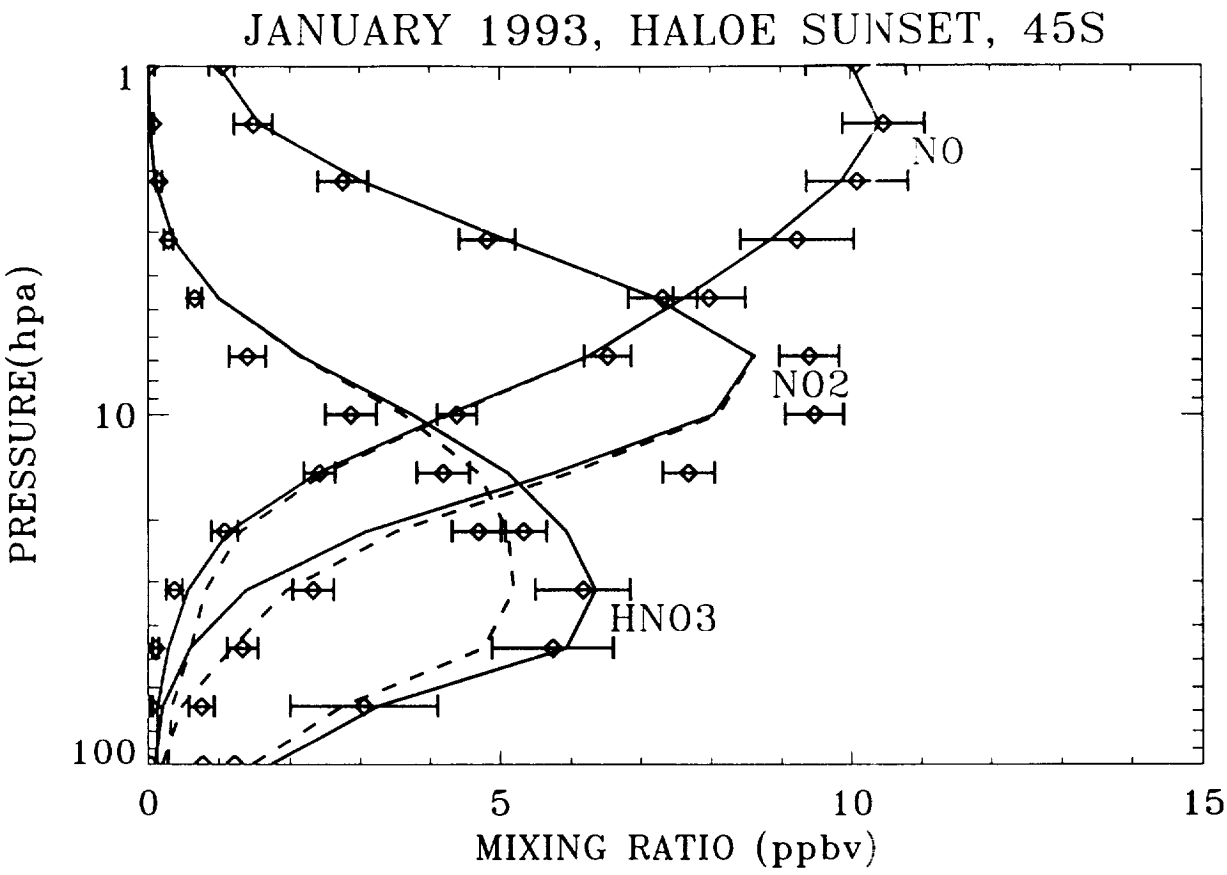
JANUARY 1993, HALOE SUNSET, 45S
PRESSURE(hpa)
1
10
100
NO
NO2
HNO3
0
5
10
15
MIXING RATIO (ppbv)

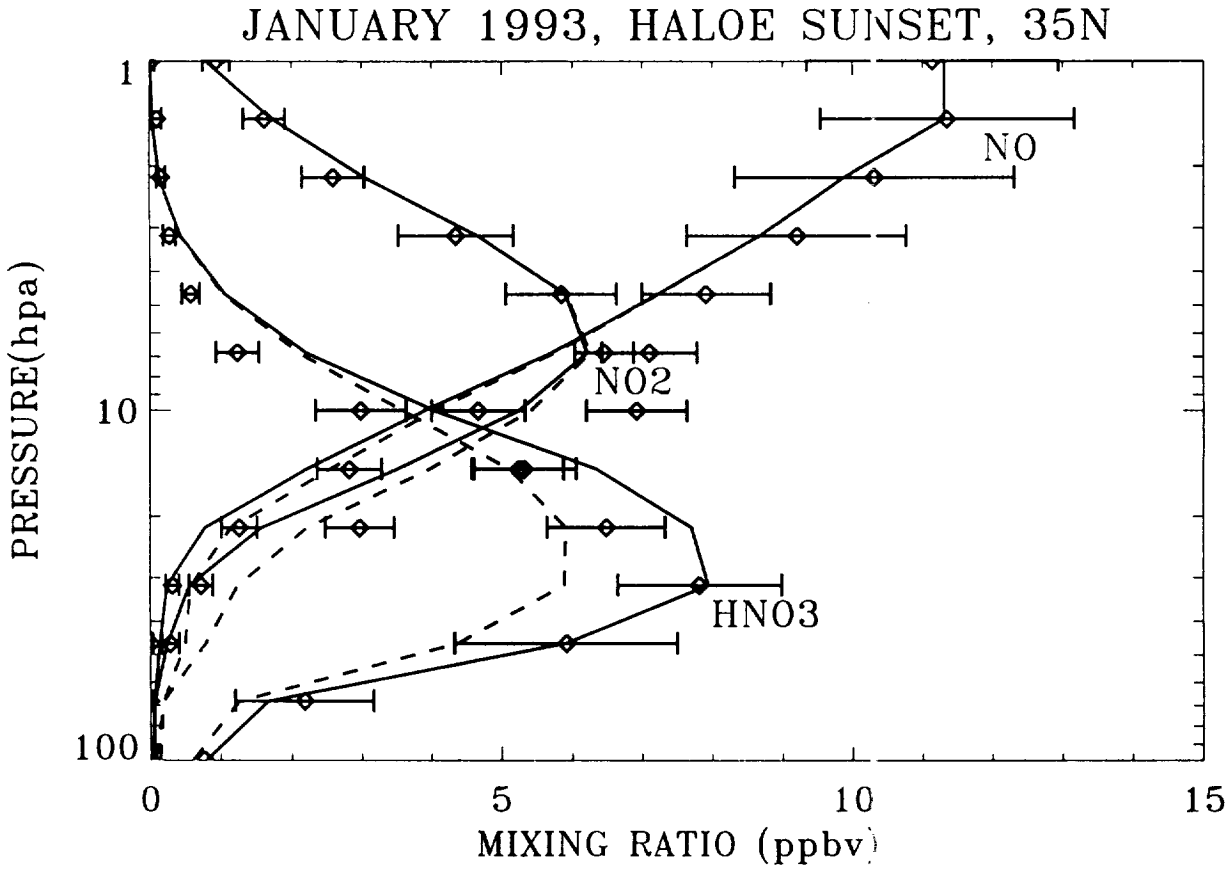
JANUARY 1993, HALOE SUNSET, 35N
PRESSURE(hpa)
1
10
100
NO
NO2
HNO3
0
5
10
15
MIXING RATIO (ppbv)

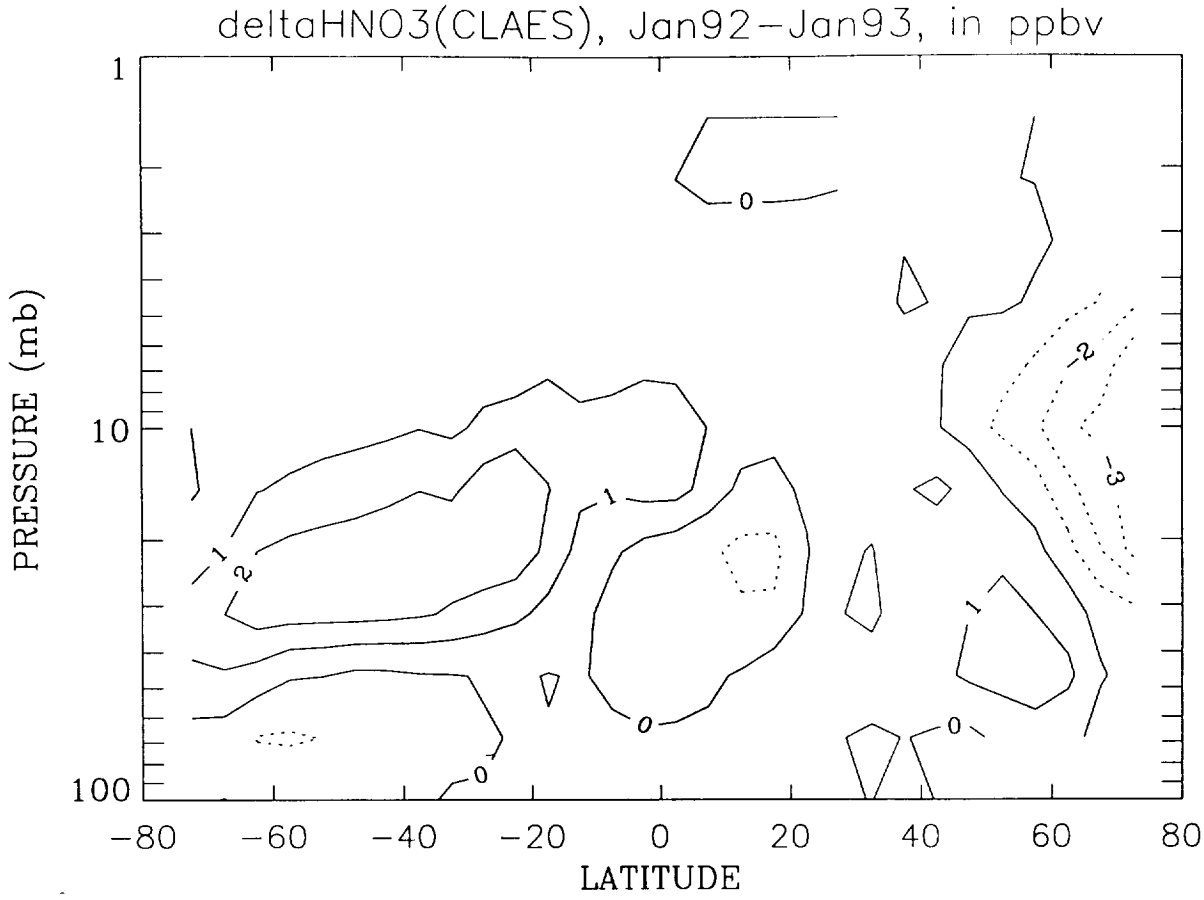
deltaHNO3(CLAES), Jan92–Jan93, in ppbv
PRESSURE (mb)
1
10
100
−80
−60
−40
−20
0
20
40
60
80
LATITUDE

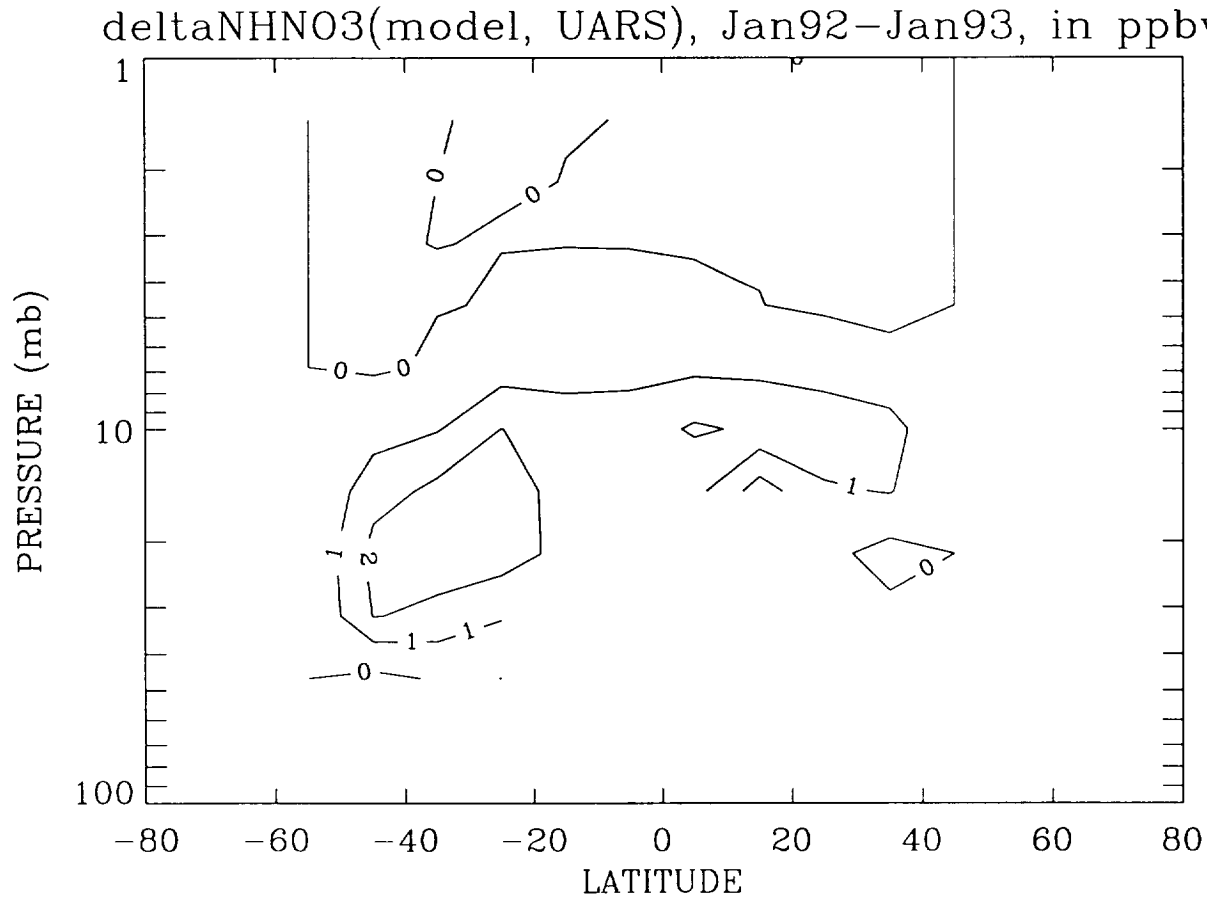
deltaNHNO3(model, UARS), Jan92–Jan93, in ppbv
PRESSURE (mb)
1
10
100
−80
−60
−40
−20
0
20
40
60
80
LATITUDE

Figure 7.

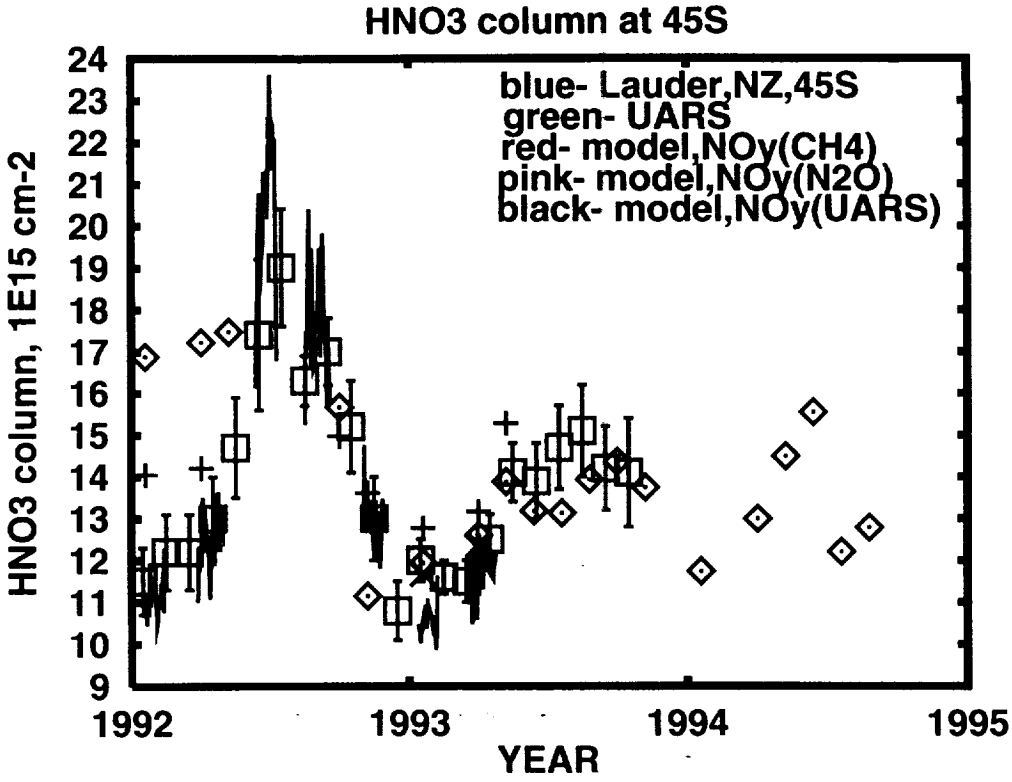
HNO3 column at 45S
blue- Lauder,NZ,45S
green- UARS
red- model,NOy(CH4)
pink- model,NOy(N2O)
black- model,NOy(UARS)
HNO3 column, 1E15 cm-2
24
23
22
21
20
19
18
17
16
15
14
13
12
11
10
9
1992
1993
1994
1995
YEAR

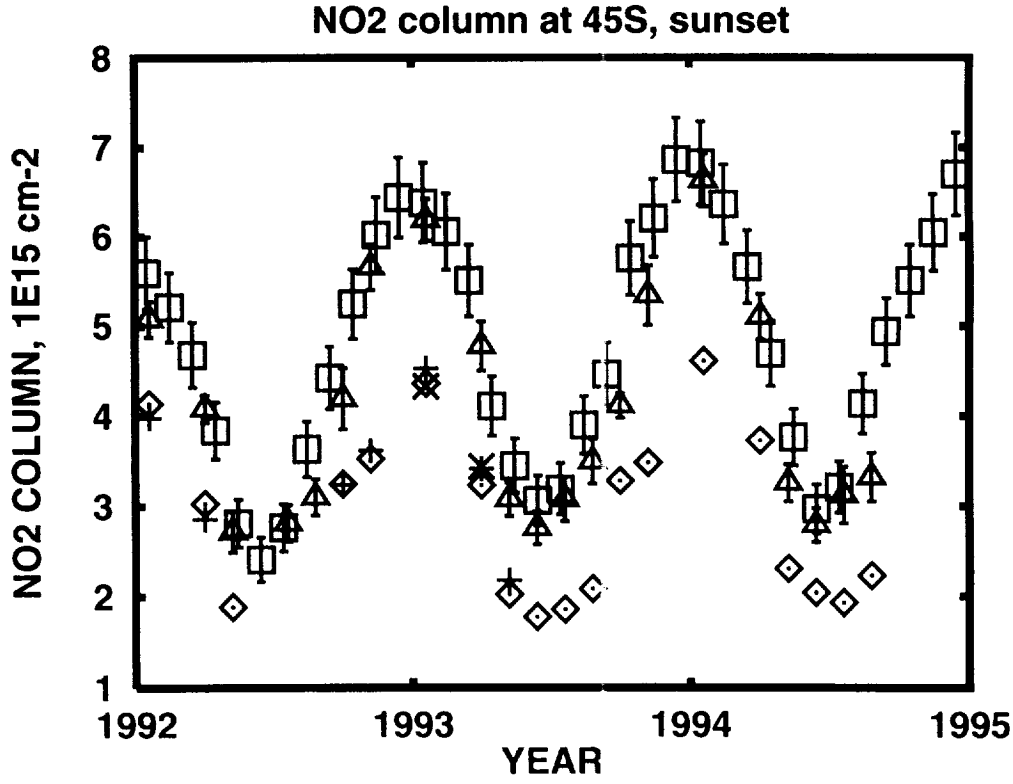
NO2 column at 45S, sunset
NO2 COLUMN, 1E15 cm-2
8
7
6
5
4
3
2
1
1992
1993
1994
1995
YEAR

FIGURE 8.

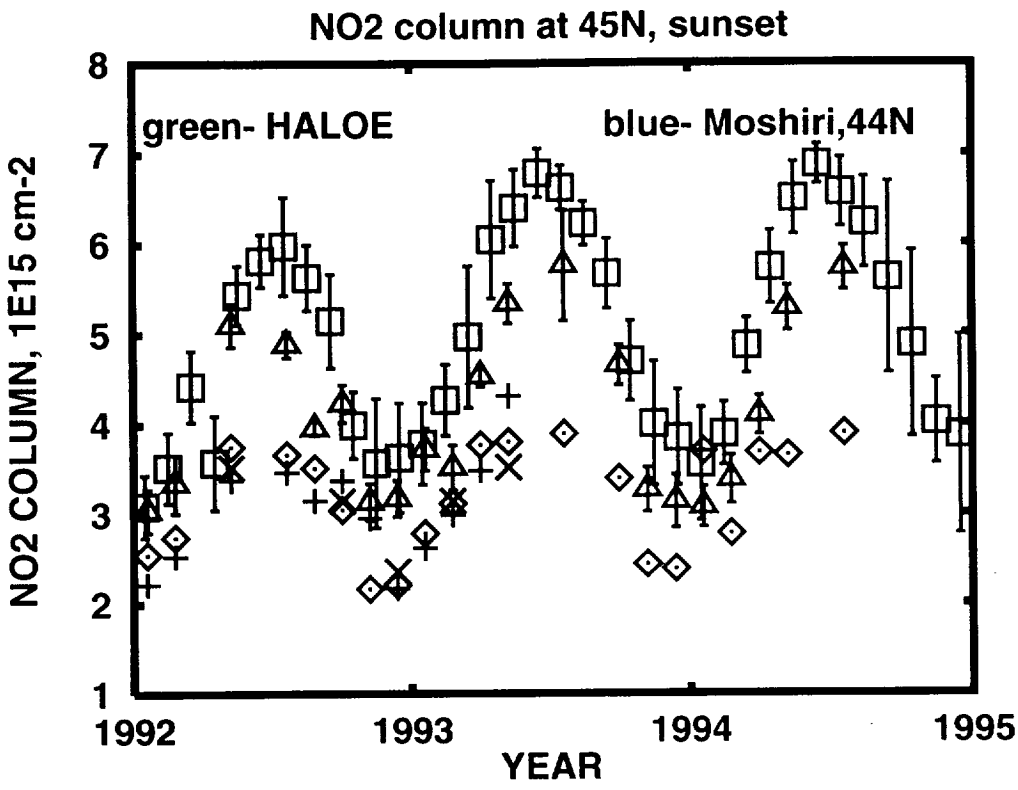
NO2 column at 45N, sunset
green- HALOE
blue- Moshiri,44N
NO2 COLUMN, 1E15 cm-2
8
7
6
5
4
3
2
1
1992
1993
1994
1995
YEAR

FIGURE 9.